RES | THE SCHOOL for RENEWABLE ENERGY SCIENCE

Setup of a test bench and testing the single solid oxide fuel cell at various temperatures

Marek Skrzypkiewicz

UNIVERSITY OF ICELAND

University of Akureyri

SETUP OF A TEST BENCH AND TESTING THE SINGLE SOLID OXIDE FUEL CELL AT VARIOUS TEMPERATURES

Marek Skrzypkiewicz

A 30 credit units Master´s thesis

Supervisors:
Prof. Umberto Desideri
Dr. David Dvorak
Prof. Thorsteinn I. Sigfusson

A Master's thesis done at
RES │ the School for Renewable Energy Science
in affiliation with
University of Iceland &
the University of Akureyri

Akureyri, February 2009

Setup of a test bench and testing the single solid oxide fuel cell at various temperatures

A 30 credit units Master's thesis

RES │ the School for Renewable Energy Science
Solborg at Nordurslod
IS600 Akureyri, Iceland
telephone: + 354 464 0100
www.res.is

Printed in 14/05/2009
at Stell Printing in Akureyri, Icelan

ABSTRACT

Solid Oxide Fuel Cells (SOFCs) are a promising source of electricity. They are efficient devices that allow direct harnessing the Gibbs free energy of reactions between fuel and an oxidant. The ongoing project in the Fuel Cell laboratory in Perugia, Italy is a part of their coordination with the Energy Research Center of Netherlands (ECN). This project was devoted to single SOFCs testing, which helps in understanding the influence of different circumstances on the SOFC performance. In this thesis is a detailed outline of the testing procedures and an expanded discussion of the results. The main objectives of this work were to: finish building the single SOFC test bench, create a model that allowed time and gas consumption forecasting for different tests, design the sulphur tolerance system, create a model for cell temperature evaluation, study recent scientific achievements in SOFC with special emphasis on single cells testing, prepare the laboratory testing procedures, perform the tests of the ASC2 Cell by InDEC B.V. The results are presented in graphs in the body of the work and in detailed tables as an appendix. The measurements gave results worse than expected, but the temperature dependence is clear. The conclusions for future development of the test bench are that the temperature measuring should be improved and software development should continue.

PREFACE

In the beginning of humankind people needed energy for heating their living spaces and cooking. They burned wood and in some areas they used other easily accessible fossil fuels like shallow coal. Since the industrial revolution, which occurred in the nineteenth century, people began to need more and more energy for industry and for households. We started to utilize every energy source it was possible to use, starting with the cheapest.

Nowadays the problem of the greenhouse effect began influencing the climate on the earth. The greenhouse effect is caused by the emission of greenhouse gases (mainly CO_2) to the atmosphere. It is stopping the radiation of heat from earth and this causes the global warming phenomenon to occur.

Thirty, forty years ago this problem did not have a significant influence on the world's climate yet. But the last few years a lot of warnings have been constantly stated that the climate is changing with an increasing speed.

In his publication "Energy in transition" (1991), J.P. Holdren states that we are not running out of energy sources in an absolute sense, nor of the possibilities to transform them, but we are running out of the cheap oil and natural gas that powered much of the growth of modern industrialized societies, the environmental capacity to absorb the impacts of burning coal and we are running out of public tolerance for the risks of nuclear fission.

Currently there is an increasing trend for reducing human emissions of CO_2 and other greenhouse gases to the atmosphere. This change can be done by the development of a so called sustainable society that will live and last without degrading the environment.

There are different options for reducing the CO_2 emissions.

The first of these could be increasing energy efficiency, which would allow reducing the fossil fuels consumption.

The next one could be switching to fuels with lower carbon to hydrogen (C:H) composition ratio. For example the typical coals C:H ratio is 8:4, oil 2:4, methane 1:4 and hydrogen 0:1. During the burning of fuels with low C:H ratio the exhaust gases consist of mainly water vapor and a smaller quantity of carbon dioxide. The emitted H_2O vapor would join the existing H_2O natural circuit and have little to no influence on the earth.

Another option is introducing hydrogen as a fuel worldwide. This means that cars, ships and other machines fueled with petroleum derivatives (gasoline, diesel and others) could be substituted with the "zero emission" machines that utilize hydrogen and air, and emit only water vapor.

Carbon capture and sequestration is also being investigated as a possible way to reduce CO_2 emissions. This is, however, a new field of research and many fears have not yet been dispelled about these technologies.

One of the most interesting directions in reducing CO_2 emissions is the development of Renewable Energy Sources such as wind, sun, hydro, geothermal heat, tidal and other "clean" energies. The energy harvested this way has very little emissions. Renewable energy sources are a promising future for the world. Humankind needs much less energy than is possible to harvest from Renewables.

Fortunately these ideas do not strongly rely on each other. They could be executed at the same time but development of each of them would catalyze faster improvements in the

others (i.e. switching to hydrogen fuels with the renewable energy sources as the source of energy for water electrolysis as a hydrogen source or generating hydrogen from natural gas with carbon dioxide capture and sequestration).

As professor Thorsteinn I. Sigfusson states in his book "Planet hydrogen – the taming of the proton" (2008): "With the advent of fuel cells, hydrogen can be harnessed in a way which makes the efficiency much higher than in the case of the Carnot era where hydrogen containing compounds were burned and their combustion energy utilized by some sort of effectively "moving a piston". By using the revolutionary fuel cell a step is taken into a post-Carnot energy era; from burning to utilization of the free energy of the electrons."

Fuel cells (FCs) are the most efficient and environmentally friendly (and therefore promising) devices generating electricity from different fuels. High temperature FCs (as i.e. Solid Oxide Fuel Cells) have an especially good chance of becoming a common way of substituting turbines and electric generators in the power plants of the future.

This thesis project is a Master of Renewable Energy Science thesis, prepared as a final component of master studies at RES | the School for Renewable Energy Science in Akureyri, Iceland. The experiments and consultations, as well as most of the writing, took place in Perugia, Italy in the Fuel Cell lab – part of Univeristy of Perugia, Faculty of Engineering.

It aims to develop a test bench for testing single Solid Oxide Fuel Cells. Within this project an ASC2 cell by InDEC B.V. was tested in five different temperatures.

It was done under direct supervision of Professor Umberto Desideri from the University of Perugia, with the assistance of Giovanni Cinti – the director of the Fuel Cell laboratory. Remote advisors were David Dvorak and Thorsteinn I. Sigfusson.

Special thanks to: *Björn Gunnarsson, Thorsteinn I. Sigfusson, David Dvorak, Umberto Desideri, Giovanni Cinti, Arnbjörn Olafsson, Sigrún Lóa Kristjánsdóttir, Paulina Sokołowska, Zbigniew, Barbara, Agata, Michał Skrzypkiewicz, Michał Pachocki, Katarina Kamenska, other RES 2008 students*.

This work is a small step in the journey to the better, energetically sustainable world.

TABLE OF CONTENTS

LIST OF FIGURES

LIST OF TABLES

1 OBJECTIVES OF THIS WORK

This work was done as a part of the project called internally "ECN" in the Fuel Cell laboratory in Perugia (part of the University of Perugia, Italy, Faculty of Engineering). This project is devoted to single Solid Oxide Fuel Cells (SOFCs) testing. Performing tests of SOFC single cells helps to understand the influence of different circumstances on the SOFC performance.

The main objectives of this work were to:

- Finish building the single SOFC test bench.
- Create a "Single Solid Oxide Fuel Cell test bench model" that will allow time and gas consumption forecasting. The procedures for different tests should be included in this spreadsheet.
- Design the sulphur tolerance system (calculate the needed container H_2S in H_2 concentration and volume, choose the Mass Flow Controller for this mixture).
- Create an "Average Cell Temperature model".
- Read the recent scientific achievements in SOFC with special emphasis on single cells testing.
- Write necessary procedures (gas supply, start-up, PC and electronic devices configuration, applying weight, cool-down).
- Launch all parts of the test bench separately and finally launch the whole test bench and show that the procedures are written correctly.
- Perform the tests and drive the conclusions for future development of this test bench.

2 HOW DOES A FUEL CELL WORK?

2.1 General idea

A fuel cell (FC) is a device that produces electricity by electrochemical reaction of a fuel and an oxidant. In a basic Hydrogen – Oxygen fuel cell the oxidant is O_2 and the fuel is H_2. The H_2 – O_2 fuel cell releases pure H_2O, electricity and heat treated as a waste but in many cases this heat can be harvested to increase the efficiency of the FC system. The idea of a FC as a "black box" is shown in Figure 2.1.1 below.

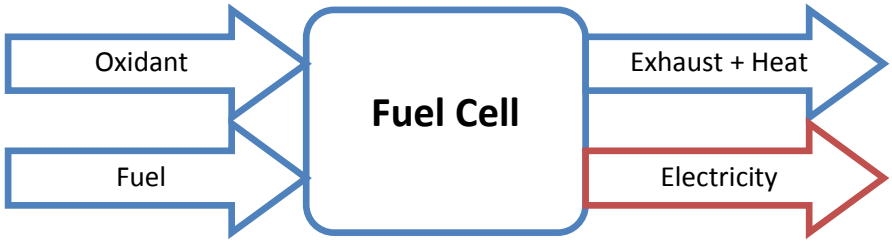

Figure 2.1.1 Fuel cell as a "black box".

2.2 Invention of a Fuel Cell

The first fuel cell was constructed by William Robert Grove in the year 1839. He constructed a device that could electrolyze water without any electricity source. His device (see Figure 2.2.1 below) worked in such a way that hydrogen (Hy) and oxygen (Ox) gases were in the test-tubes above the four lower beakers. These gases reacted in a sulfuric acid solution and formed H_2O. During this electrochemical reaction the electrons were released and they electrolyzed water in the upper reservoir to O_2 and H_2 using a catalyst metal as the electrodes.

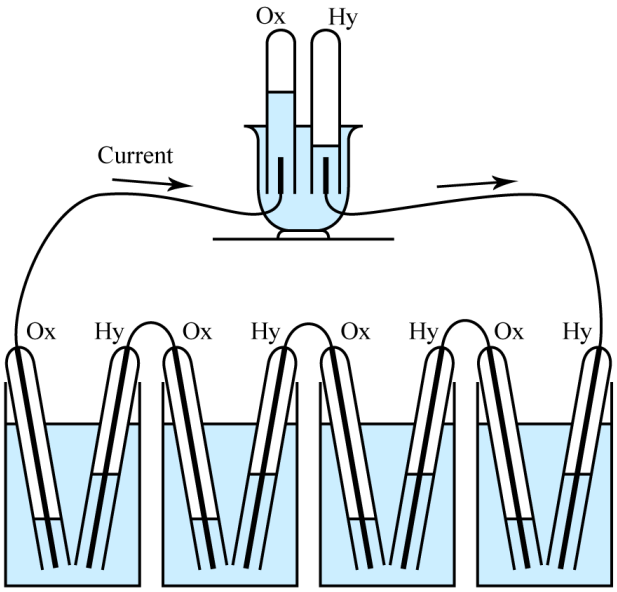

Figure 2.2.1 Grove's Gaseous Voltaic Battery. Source: Wikipedia.org; open source.

2.3 Modern FC structure

Modern fuel cells consist of three main parts: anode, electrolyte and cathode. They are manufactured in the form of three different layers connected to each other. Each of them has high influence on the cell's performance. The scheme of a Proton Exchange Membrane Fuel Cell (PEMFC) is shown in Figure 2.3.1 below.

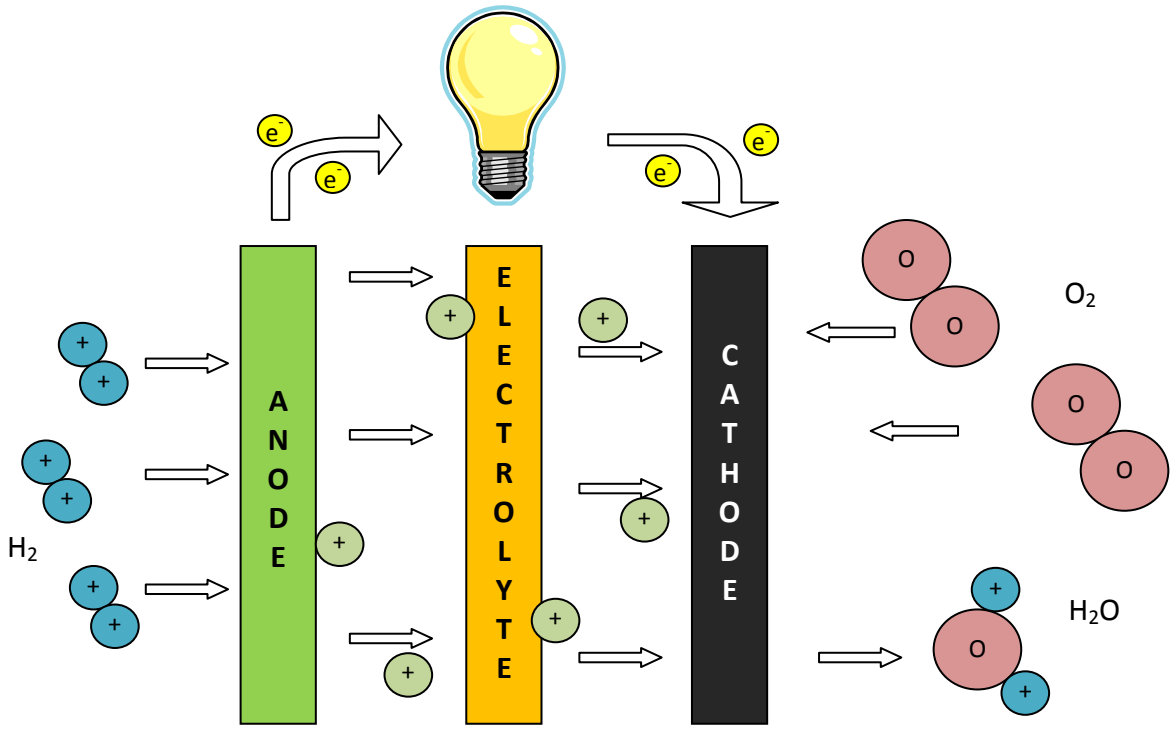

Figure 2.3.1 Proton Exchange Membrane Fuel Cell scheme.

Hydrogen (H_2) molecules are supplied to the anode. The Anode catalyzes the hydrogen molecule decomposition into protons and the electrons are released. It is possible because the next part of a FC is the electrolyte, which does not conduct electrons but allows protons to get through to the cathode side. The cathode catalyzes oxygen decomposition to let it react with the protons incoming through the electrolyte to form water. The electrons do the work (the light bulb lights) because of the electronic potential difference between cathode and anode, which actually pulls electrons through the light bulb.

Besides water and electric power the by-product of a FC is heat, which comes mainly from losses in activation, transport of protons and electrons (ohmic losses) and transport of the reactants.

The PEMFC was discussed above only to show the general concept of fuel cells. This thesis concentrates on Solid Oxide Fuel Cells (SOFCs); therefore the rest of this work will concentrate on SOFCs.

2.4 How does a solid oxide fuel cell work?

In principle a SOFC is also a fuel cell, so when analyzed generally, works as shown in Figure 2.1.1 above. Although the general idea the same as for a PEMFC, the SOFC works in a slightly different manner than the PEMFC. In a proton exchange membrane fuel cell the electrolyte conducts protons and does not conduct electrons or oxygen ions.

The SOFC has an electrolyte that conducts oxygen ions known as O^{--}. which is also described as O^{2-}. The difference between PEMFC and SOFC is in the location of the H_2O creation. A PEMFC releases water on the cathode side whereas SOFC releases water on the anode side, where the O^{--} ions react with the fuel supplied. The concept of a SOFC is shown in Figure 2.4.1 below.

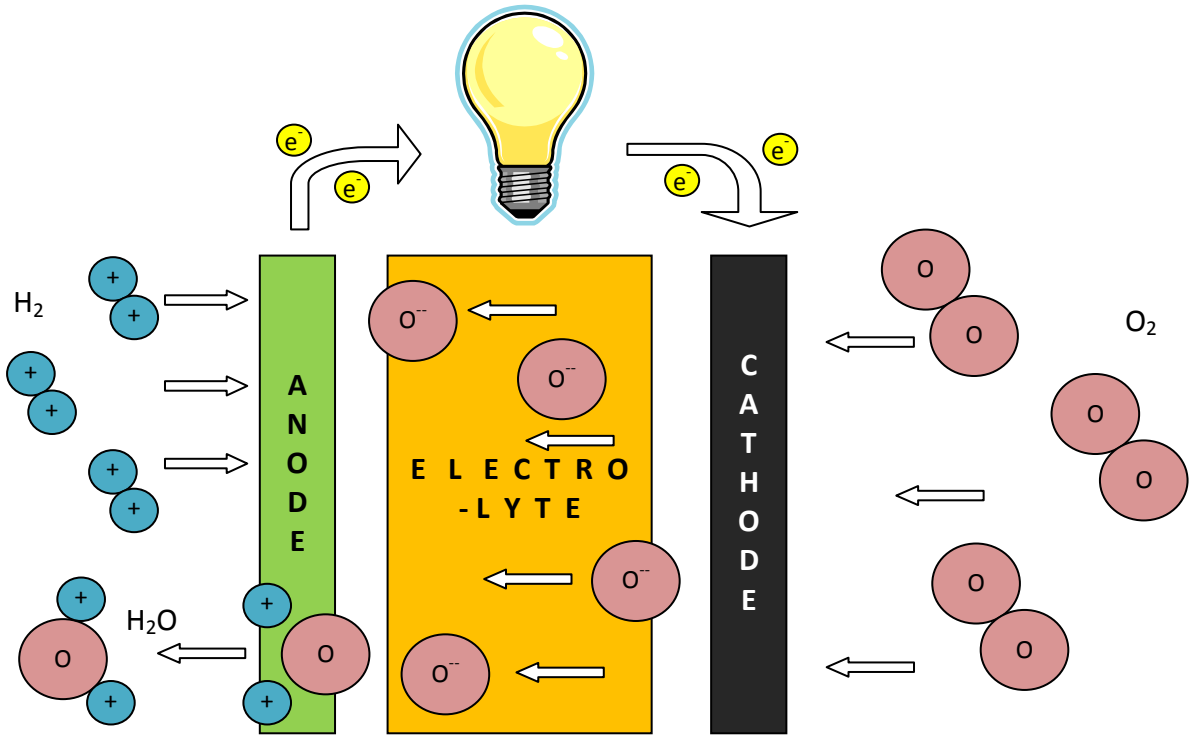

Figure 2.4.1 Solid Oxide Fuel Cell scheme.

A thin ceramic membrane is used as an electrolyte in SOFCs. To obtain a high-enough ionic conductivity of the membrane, a high temperature is needed. Currently a lot of research is being done to test new materials for electrolytes, anodes and cathodes to substitute them with better ones. The materials issue will be discussed later, in paragraph 2.5 below.

SOFCs are very often still called High Temperature Fuel Cells (HTFC), although recently the performance of SOFCs has been shown even below 500 °C (SUN Xueli et al, 2006, see Figure 2.5.6, page 9).

FCs are devices with electrochemical reactions occurring on the surfaces of the anode and cathode. For $H_2 – O_2$ SOFC the anode and cathode half reactions are:

$H_2 + O^{--} \rightarrow H_2O + 2e^-$ for the anode and

$½O_2 + 2e^- \rightarrow O^{--}$ for the cathode

The main advantages of solid oxide fuel cells are, according to Ryan O'Hayre et al. (2006):

- Fuel flexibility
- Non-precious metal catalyst
- High quality waste heat for cogeneration applications
- Solid electrolyte
- Relatively high Power Density (PD, W/cm^2)

I would add as well higher efficiency compared to FCs working in lower temperatures.

The disadvantages are:

- Significant high-temperature materials issues
- Sealing issues
- Relatively expensive components/fabrication

Solid Oxide Fuel Cells are therefore promising devices for applications in households and power plants of the future. They would offer an efficient electrical energy source and the waste heat is of high quality for heating houses or co-generation in power plants.

2.5 Development of the materials for electrodes and electrolyte

A Solid Oxide Fuel Cell is a multilayer structure consisting of three main layers shown in Figure 2.5.1 below:

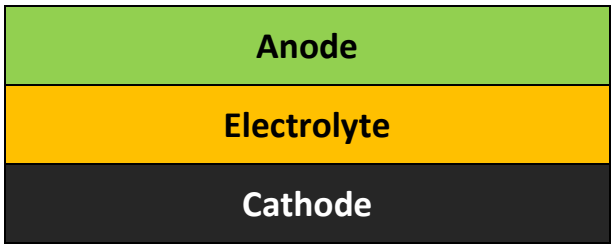

Figure 2.5.1 Solid Oxide Fuel Cell structure

The anode is the place where fuel enters the cell. The fuel can be hydrogen gas, but could be also other fuels like i.e. methane or ethanol. In this place the fuel is oxidized with the oxygen ions O^{--} that come to the anode through the electrolyte. Anode material should have a high catalytic activity for the Fuel oxidation. Its microstructure should provide a large number of Triple Phase Boundaries (TPB's) on which the electronic conductive electrode, ionic conductive electrolyte and fuel meet each other. Another important feature of the anode should be its porosity to allow the fuel gas to be transported from the manifold to the TPB's.

The cathode material's features in the assumptions should be very similar to anode. The only difference is the catalytic abilities of splitting O_2 particles to O^{--} ions.

The electrolyte should be a layer that prevents electrons passing and allows ions to be transported. It should be a so called purely ionic conducting membrane. The important parameter here is the ionic conductivity.

All these layers should have a well known and adjusted thermal expansion coefficient, interfaces of the contacting materials should be chemically compatible and the materials should be chemically stable in the atmospheres possible to obtain during SOFC operation, including possible leakages as well.

André Weber and Ellen Ivers-Tiffée (2004) say that state-of-the-art materials currently used in most SOFC systems are Yttria Stabilized Zirconia (YSZ) as the electrolyte, which can be either TZP (3YSZ: ZrO_2 doped with ~3 mol% Y_2O_3) or CSZ (8YSZ: ZrO_2 doped with ~8 mol% Y_2O_3). The ionic conductivity of TZP is significantly lower but this material is advantageous because of its outstanding mechanical stability. Strontium doped lanthanum manganite (LSM) is used as the cathode and nickel/YSZ cermets as the anode.

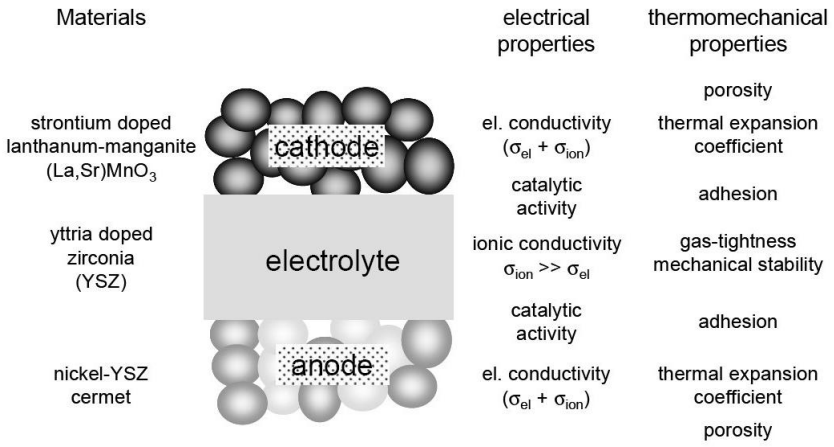

Figure 2.5.2 State of the art materials and required electrical and (thermo) mechanical properties of SOFC-single cells. Source: André Weber, Ellen Ivers-Tiffée, 2004.

It is known (André Weber, Ellen Ivers-Tiffée, 2004) that the cathode governs the main part of the losses. The transport of oxide ions within the electrode material is advantageous concerning the number of possible reaction pathways. Therefore electrodes should be either a composite consisting of an electronic and an ionic conducting phase or a mixed conducting metal oxide to enlarge the active area into the electrode volume, as shown in Figure 2.5.3 below.

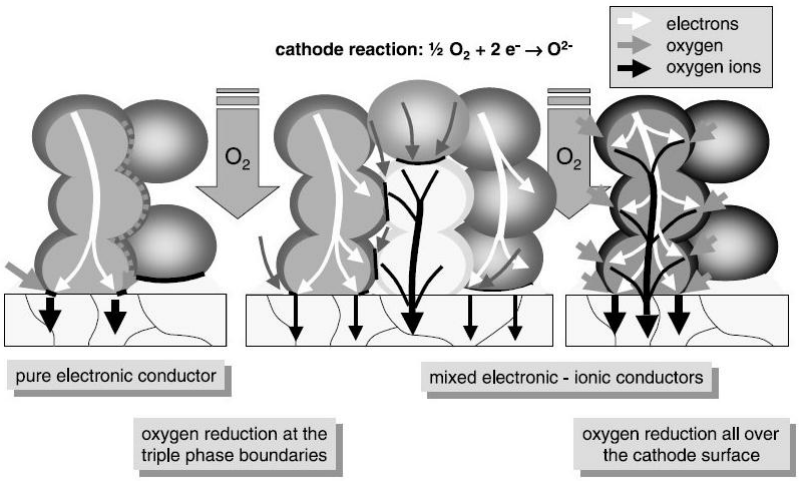

Figure 2.5.3 Oxygen reduction at a pure electronic, composite and mixed conducting cathode. Source: André Weber, Ellen Ivers-Tiffée, 2004.

For example, in the $La_{0.8}Sr_{0.2}Mn_{1-x}Co_xO_3$ solid solution (LSMC), the electrical and oxygen ion conductivity can be increased significantly by substituting a part of the manganese with cobalt (B.C.H. Steele, 1996). Such a cathode would have a decreased polarization resistance, which would result in lowering the losses. Unfortunately a high amount of cobalt increases the thermal expansion coefficient, which results in the cathode/electrolyte delamination after thermo-cycling of the cell.

One way to prevent delamination of the cathode/electrolyte interfaces is to apply the metal organic deposition (MOD) (D. Herbstritt, et al. 1999) technology for applying nanoporous thin film cathodes. Figure 2.5.4 below shows the details of the MOD technology as well as the YSZ particles screenprinting idea.

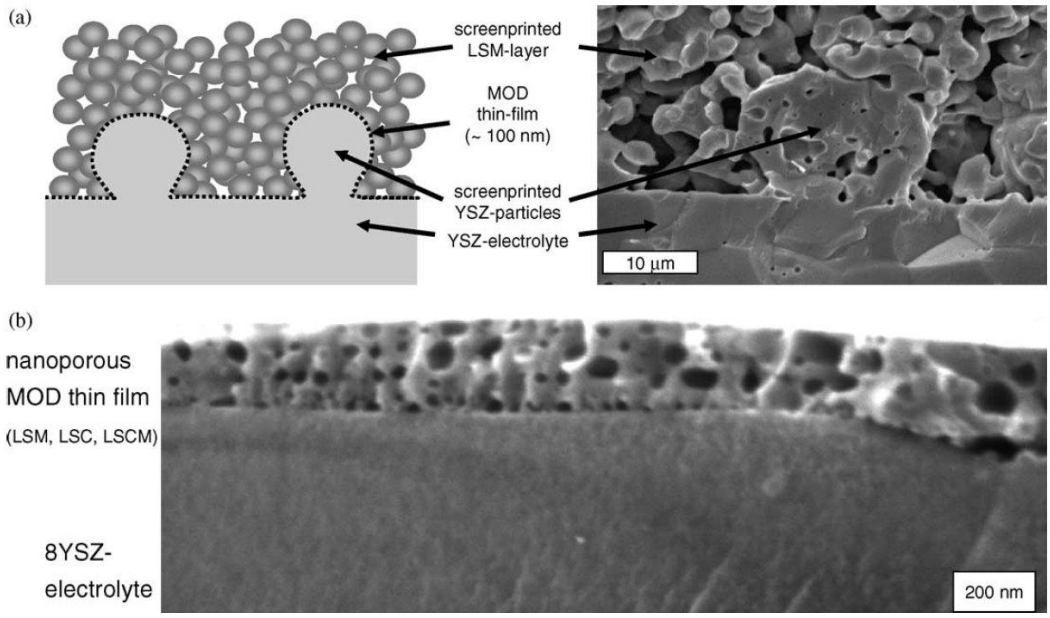

Figure 2.5.4 Improved cathode/electrolyte interface: the effective electrolyte surface area is enlarged by (a) structuring the substrate surface with screenprinted 8YSZ particles; (b) coating the whole electrolyte surface with a nanoporous electrochemical active MOD. Source: André Weber, Ellen Ivers-Tiffée, 2004.

Such an interface is a delamination-proof in the case of thermo-cycling compared to a standard monolayer cathode cell.

Another obvious possibility for increasing the performance of the cell at intermediate/low operating temperatures is reducing the electrolyte thickness. It is done by manufacturing anode or cathode supported cells. The concepts are shown in Figure 2.5.5 below.

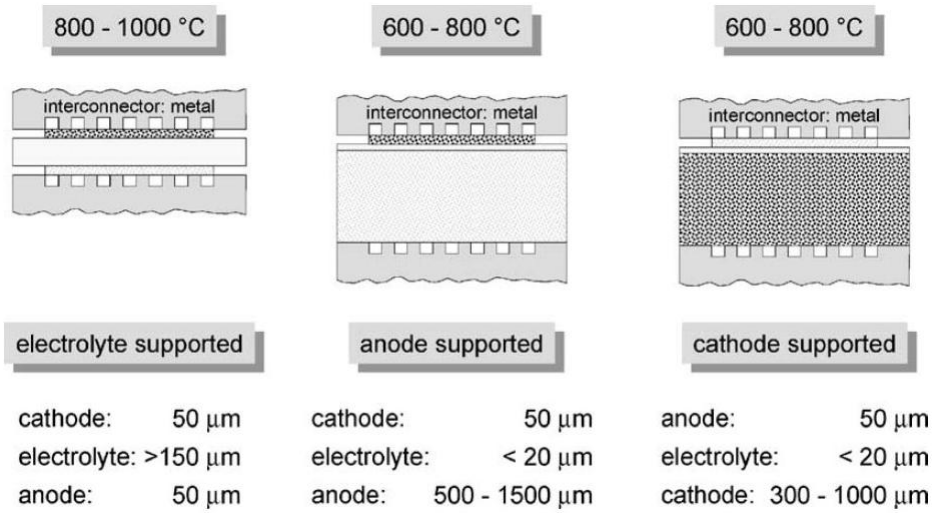

Figure 2.5.5 Planar single cell concepts. Source: André Weber, Ellen Ivers-Tiffée, 2004.

The most popular is the anode supported SOFC, manufactured by InDEC B.V./H.C Starck, Allied Signal, FZ-Jülich and many others.

Lately the topic of interest is the Low Temperature SOFC. SUN Xueli et al. (2006) discovered a new cathode material - $SmVO_4$ that, with a GdSmCeO – carbonate 0,2 mm

thick electrolyte, has interesting performance in the 450-550 °C temperature range, as shown in Figure 2.5.6 below.

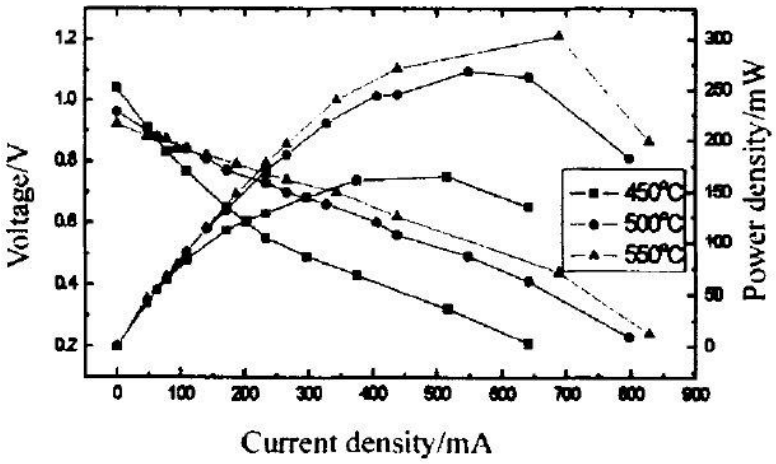

Figure 2.5.6 $SmVO_4$-cathode GdSmCeO-electrolyte, Pt-anode cell performance (see paragraph 2.6). Source: SUN Xueli et al. 2006.

2.6 Testing of Solid Oxide Fuel Cells

This branch of SOFC science is the most interesting from the point of view of this work. Many researchers (Joon-Ho Koh, et al. 2002; Futoshi Nishiwaki et al. 2006; P. Leone et al. 2008; Y.J. Leng et al. 2004; Xianliang Huang et al. 2007; Kyung Joong Yoon et al. 2007; R.N. Basu et al. 2008) concentrate their research on performing tests of single solid oxide fuel cells. Usually these works contain three main parts:

- Cell fabrication: what are the materials, how it was manufactured – detailed specification of manufacturing every layer (Anode, Electrode, Cathode and sometimes the interlayers)
- Cell testing: Usually j-V curves (Current Density [A/cm^2] – Voltage [V]) (also called polarization or performance curves) are performed in different temperatures, along with Power Density (PD) curves. Some of the papers include Electrochemical Impedance Spectroscopy (EIS) measurements.
- Microstructural Characterization: usually the researchers who fabricate their cells in their lab using sophisticated materials and new technologies examine the cell after the high temperature test in a SEM (Scanning Electron Microscope). The result is a SEM micrograph showing the cell structure. An example of such a SEM micrograph is in Figure 2.6.1 below.

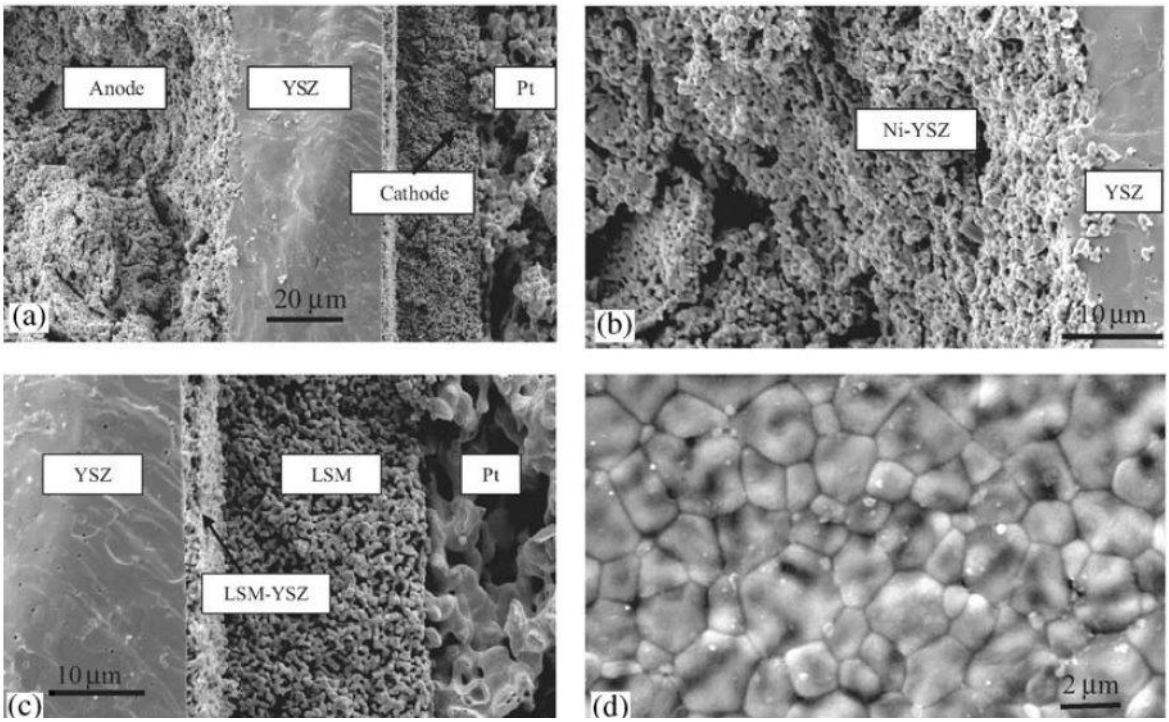

Figure 2.6.1 SEM micrographs of the cross section of: (a) fractured cell; (b) part of anode; (c) double-layer cathode and (d) the top view of YSZ electrolyte film. Source: Y.J. Leng et al. 2004.

2.7 Numerical modeling of SOFC.

Numerical modeling of the Solid Oxide Fuel Cells can be done by modeling the system or the fuel cell itself.

Within this work the Single SOFC Test Bench Model has been created. This model is described in paragraph 5.2 on page 38. The main purpose of preparing this model is to allow fast estimation of the time and needed amount of gases for the tests. It also contains the set of procedures for each possible way to perform test.

In the next chapter the basic idea of cell modeling is presented.

The situation (chemical state, mass balance, charge balance etc.) inside a SOFC cell can be described by equations in differential forms, of which the most important are the equations in Table 2.7.1 below:

Table 2.7.1 Typical governing equation considered in each SOFC component, Source: Sadik Kakaç et al. 2007.

Fuel cell evaluation				
Actual cell voltage [1,13,16–18,20]	$V = E_{\mathrm{Th}} - \eta_{\mathrm{act}} - \eta_{\mathrm{ohm}} - \eta_{\mathrm{conc}}$			
Equations	Channels	Electrodes	Electrolyte	Interconnects
Conservation of mass	$\frac{\partial \rho}{\partial t} + \nabla \cdot (\rho \mathbf{V}) = S_{\mathrm{m}}$	$\frac{\partial}{\partial t}(\rho\varepsilon) + \nabla \cdot (\rho\varepsilon \mathbf{V}) = 0$		
Conservation of momentum	$\frac{\partial}{\partial t}(\rho \mathbf{V}) + \nabla \cdot (\rho \mathbf{V}\mathbf{V}) = -\nabla p + \rho\vec{g}\nabla \cdot \vec{\tau} + \vec{S}_M$	$\frac{\partial}{\partial t}(\rho\varepsilon \mathbf{V}) + \nabla \cdot (\rho\varepsilon \mathbf{V}\mathbf{V}) = -\varepsilon\nabla p + \nabla \cdot (\varepsilon\zeta) + \frac{\varepsilon^2 \mu \mathbf{V}}{\kappa}$		
Species balance	$\frac{\partial}{\partial t}(\rho c_i) + \nabla \cdot (\rho \mathbf{V} c_i) = -\nabla \cdot \vec{J}_i + S_{s,i}$	$\frac{\partial}{\partial t}(\rho\varepsilon c_i) + \nabla \cdot (\rho\varepsilon \mathbf{V} c_i) = -\nabla \cdot \varepsilon\vec{J}_i + S_{\mathrm{s},i}$		
Conservation of energy	$\frac{\partial}{\partial t}(\rho e) - \frac{\partial p}{\partial t} + \nabla \cdot (\rho \mathbf{V} e) = \nabla \cdot (k^{\mathrm{eff}} \nabla T) + S_{\mathrm{e}} + S_{\mathrm{rad}}$	$\frac{\partial}{\partial t}(\rho\varepsilon e) - \varepsilon\frac{\partial p}{\partial t} + \nabla \cdot (\rho\varepsilon \mathbf{V} e) = \nabla \cdot \varepsilon\left(k_{\mathrm{eff}} \nabla T - \sum_i h_i \vec{J}_i\right) + S_{\mathrm{e}} + S_{\mathrm{rad}}$	$\frac{\mathrm{d}}{\mathrm{d}x}\left(-A_{\mathrm{e}} k_{\mathrm{e}} \frac{\mathrm{d}T_{\mathrm{e}}}{\mathrm{d}x}\right)\Delta x = q_{\mathrm{e-ele,a}} + q_{\mathrm{e-ele,c}} + q_{\mathrm{conv,ele,a}} + q_{\mathrm{conv,ele,c}} + q_{\mathrm{rad,e}} + q_{\mathrm{gen,e}} + q_{\mathrm{e,joule}}$	$\frac{\mathrm{d}}{\mathrm{d}x}\left(-A_{\mathrm{int}} k_{\mathrm{int}} \frac{\mathrm{d}T_{\mathrm{int}}}{\mathrm{d}x}\right)\Delta x = q_{\mathrm{int-ele}} + q_{\mathrm{conv,chan}} + q_{\mathrm{rad,chan}} + q_{\mathrm{gen,int}} + q_{\mathrm{int,joule}}$
Ohm's law			$j_{\mathrm{io}} = -\sigma_{\mathrm{io}}^{\mathrm{eff}} \nabla \phi_{\mathrm{io}}$	$j_{\mathrm{el}} = -\sigma_{\mathrm{el}}^{\mathrm{eff}} \nabla \phi_{\mathrm{el}}$
Conservation of charge			$\nabla \cdot (\sigma_{\mathrm{io}}^{\mathrm{eff}} \nabla \phi_{\mathrm{io}}) = S_{\mathrm{io}}$	$\nabla \cdot (\sigma_{\mathrm{el}}^{\mathrm{eff}} \nabla \phi_{\mathrm{el}}) = S_{\mathrm{el}}$
Charge balance				$\nabla \cdot j_{\mathrm{io}} = -\nabla \cdot j_{\mathrm{el}}$

These differential equations can be discretized using common methods and solved numerically. According to Sadik Kakaç et al. (2007) there are 4 main ways of discretization and solution of a numerical problem:

1. Taylor-series formulation: the finite-difference equations are derived via a truncated Taylor series. The finite difference approximations of the derivatives of unknowns are replaced in all derivatives appearing in the governing equations yielding an algebraic equation for unknowns at each grid point.

2. Variational formulation: this formulation is very commonly employed in the finite-element (FE) methods for stress analysis. The calculus of variations shows that solving certain differential equations is equivalent to minimizing a related quantity called the functional.

3. Method of weighted residuals: the simplest weighting function is W = 1. The calculation domain will be divided into subdomains or control volumes and a number of weighted residual equations can be generated. This variant of the method of weighted residuals is called the subdomain method or the control-volume formulation.

4. Spectral methods: these methods approximate the unknowns by means of truncated Fourier series or a series of Chebyshev polynomials. Unlike the finite difference or FE approach the approximations are not local but valid throughout the entire computational domain. The constraint that leads to the algebraic equation for the coefficients of these series is provided by weighted residuals or by making the approximate function coincide with the exact solution at a number of grid points.

The numerical modeling of Fuel Cells leads to better understanding of the processes inside cells and stacks. The temperature profile and heat transfer help the researchers manufacture the cells so that they can tolerate faster temperature changes. Modeling of the channels helps to increase the fuel utilization factor. Applying modeling in fuel cells design results in improving their performance.

2.8 SOFC Systems

Besides the development of the cells' materials and design, there are efforts being made toward modeling the whole SOFC systems. Some of these concepts were actually realized – they have been constructed and are in operation. It is a very interesting topic, because it shows the pathways for the development of the world largest energy facilities. It is already possible to build a SOFC power plant which is much more environmentally friendly than a traditional one (with heat engine and electric generator). The issues which need to be addressed are the cost of the SOFC system and its durability.

Ph. Hofmann et al. (2007) investigated a real system in which a planar high temperature Ni-GDC/YSZ/LSM SOFC was operated successfully for 150 h on wood gas from an existing two-stage biomass gasifier. The wood gas pre-treatment included scavenging of sulphur and tar species as well as moderate humidification to achieve a Steam to Carbon ratio (S/C) equal 0,5. The experimental procedure strengthens the purpose of proving that the technological concept of feeding gas derived from a biomass gasifier into a SOFC is feasible (Ph. Hofmann et al. 2007).

Their system gave results as seen in Figure 2.8.1 below.

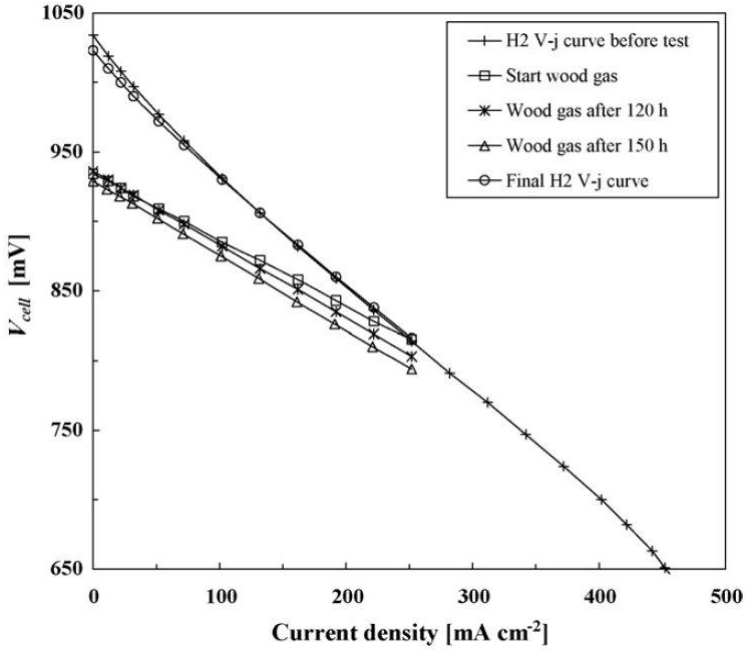

Figure 2.8.1 j-V curves on H_2 before wood gas, onset and during wood gas operation, and on H_2 after wood gas operation. Source: Ph. Hofmann et al. 2007.

No carbon deposition was noticed. It looks like the available technology is reaching the point in which the SOFC will start to be competitive on the energy market. Some of the systems like this are already working as research sites. Hopefully such systems will soon be in operation worldwide.

The other branch is the theoretical SOFC systems investigation. One of them, which is very interesting for Europe because of the available coal resources, is the one analyzed by Timo Kivisaari et al. (2007).

The purpose of their study was to find out the feasibility of integrating a 50MW fuel cell system, fed by gas from a coal gasifier, with an existing network for distribution of heat

and power. The work they presented was the result of the technical evaluation of a 50MW coal fired high-temperature fuel cell power plant. The overall system can be divided into four subsystems including: coal gasification, gas cleaning, power generation and heat recovery. The final system, an entrained flow gasifier combined with standard low-temperature gas cleanup and SOFC, resulted in an overall electrical efficiency of about 47%, and an overall efficiency close to 85% (Timo Kivisaari et al. 2007).

Table 2.8.1 Comparison of different power generation techniques. Source: Timo Kivisaari et al. 2007.

Case	BARAKA	IGCC	PFBC
Unit size (MW_e)	23.4	262	70
Electrical efficiency (% HHV)	45.1	39.7	33.2
SO_2 (g/MWh)	0.7	612.4	774.5
NO_x (g/MWh)	133.6	494.4	288.0

As can be seen in the table above, the "BARAKA" SOFC-CHP system is much more efficient and environmentally friendly compared to the most advanced systems available now.

2.9 Different designs of the Solid Oxide Fuel Cells – recent research and developments.

2.9.1 Using the catalyst layers in SOFC

The idea of using different hydrocarbon fuels in SOFC was mentioned before. The Ni/YSZ anode material has sufficient electrochemical activity for H_2 oxidation. However, Ni/YSZ suffers a number of drawbacks while using hydrocarbon fuels; notably the carbon deposition, which covers the active sites of the anodes, resulting in the rapid degradation of the cell's performance (Xiao-Feng Ye et al. 2008).

Therefore there is a need for the use of a catalyst for the direct oxidation of hydrocarbons to CO_2 on the anode side; CO_2 would escape in gaseous form. It has been proven that adding a Ru–CeO_2 surface catalyst layer allows the propane partial oxidation reaction (Z. Zhan, S.A. Barnett, 2005).

In the case of ethanol as the fuel for a SOFC it is known (Y. Xiao-Feng et al. 2007) that a Cu–CeO_2–ScSZ (Scandia stabilized zirconia) anode is a good catalyst for direct oxidation of the ethanol steam. But manufacturing this kind of anode is expensive because it needs wet impregnations and low temperature calcinations.

The newest achievement in this field is the addition of a Cu–CeO_2 catalyst layer to the supported anode surface, which yielded much better performance in ethanol fuel by internal reforming (Xiao-Feng Ye et al. 2007).

Figure 2.9.1 shows the SEM micrograph picture of the structure of a SOFC with a thin anode catalyst Cu-CeO_2 layer.

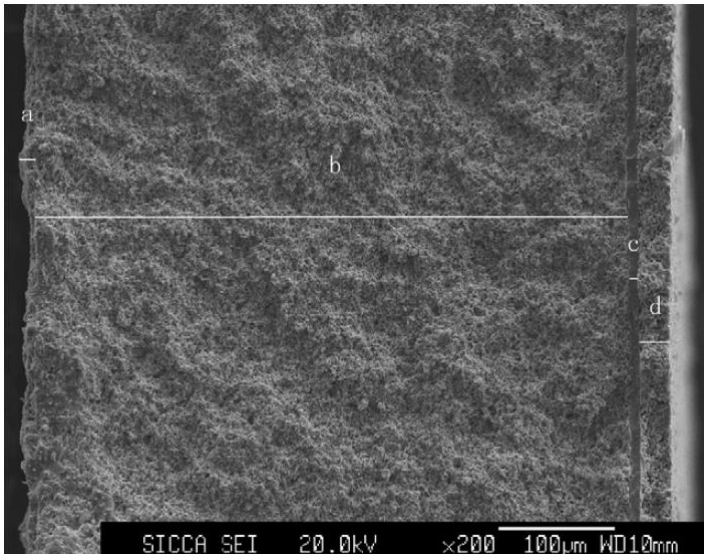

Figure 2.9.1 SEM micrograph of a fractured cell showing four layers, (a) porous Cu–CeO_2 catalyst layer, (b) porous Ni/YSZ-supported anode, (c) dense ScSZ electrolyte and (d) porous PCM cathode. Source: Xiao-Feng Ye et al. 2007.

The addition of a Cu–CeO_2 catalyst layer to the support anode surface yielded much better performance in ethanol fuel probably due to the fact that the ethanol steam reforming reaction takes place in the catalyst layer.

Cracking and delamination of the catalyst layer is the main reason for the performance degradation of cells with this two-layer structure anode. Fabrication of this structure for long-term stability continues to be a potential concern, and the conversion over ethanol feed needs to be determined in order to improve internal reforming efficiency by analyzing the exit gas later (Xiao-Feng Ye et al. 2007).

2.9.2 Composite interlayers in the electrode/electrolyte interface

Recently, application of a thin-film composite interlayer has been introduced as a means to improve the charge-transfer reaction in the electrode/electrolyte interface. By inserting interlayers, electrochemical performance was enhanced by 30% (T.L. Reitz, H. Xiao, J. 2006).

Tae Wook Eom et al. in their recent paper (2008) investigated the effect of the anode/electrolyte interlayer on cell performance and the electrolyte structure. They manufactured the cell showed in Figure 2.9.2 below.

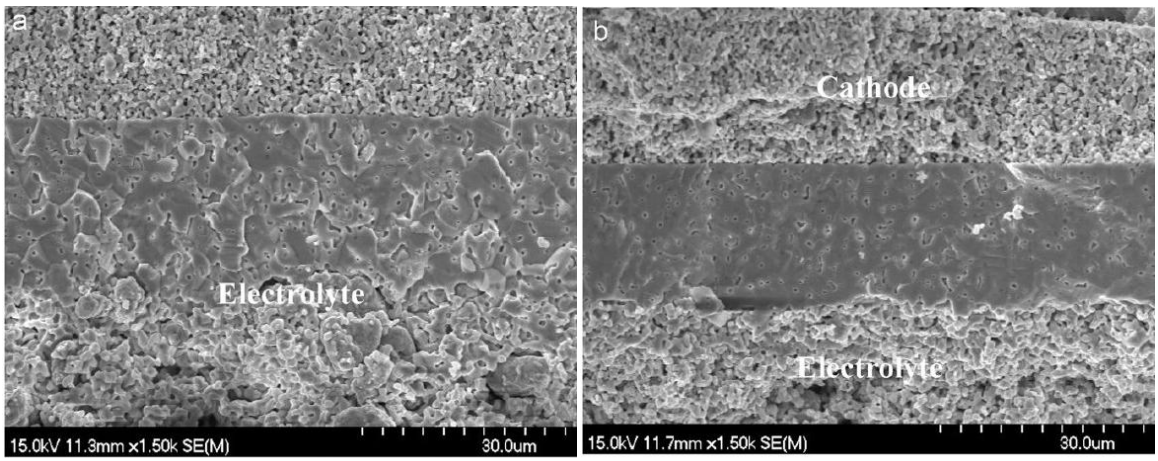

Figure 2.9.2 SEM micrograph of cross-section of SOFC: (a) SOFC without interlayer, (b) SOFC with anode interlayer. Source: Tae Wook Eom et al. 2008.

The figure shows the fabricated thin-film electrolyte SOFC single cells. The typical thickness of the anode interlayer was 10µm and that of the electrolyte layer was 30µm. In addition, it was observed that the electrolyte layer without an interlayer has more pores and cracks compared to the electrolytes with an interlayer.

Introducing the interlayer caused a performance boost for the SOFC, which is clearly visible on the obtained j-V and Power Density curves in Figure 2.9.3 below.

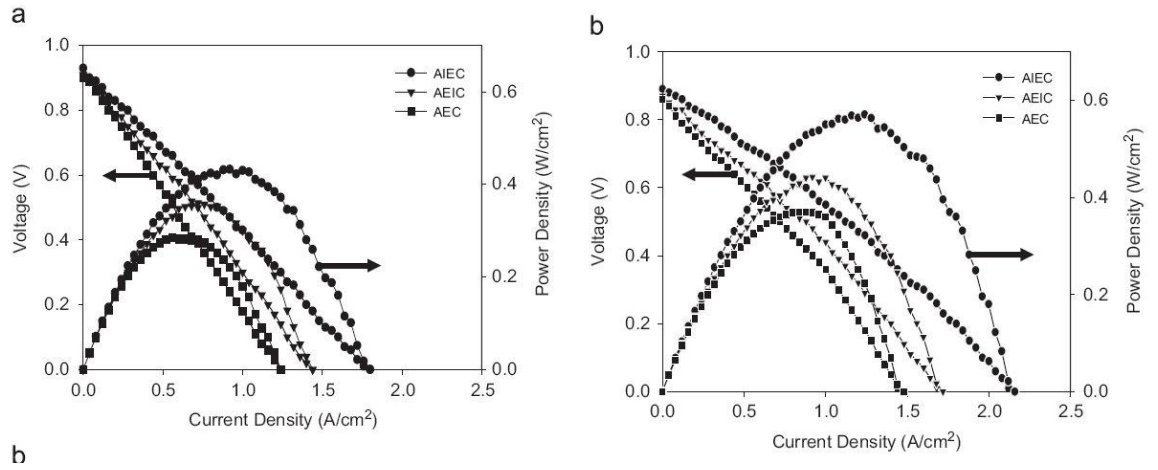

Figure 2.9.3 Performance of anode-supported single cell without interlayer, with anode interlayer, and with cathode interlayer at 700 (a), and 800 °C (b) (A: anode, I: interlayer, E: electrolyte, C: cathode). Source: Tae Wook Eom et al. 2008.

By the addition of an interlayer onto the NiO–YSZ anode, the surface Root Mean Square Roughness (RMSR) of the anode was diminished by about 40% from 621 to 377 nm and dense and crack-free electrolytes were obtained. Moreover, when the interlayer was introduced, the electrical performance was enhanced remarkably by 50% and the MPD was 0,57W/cm^2 at 800 °C and 0,44W/cm^2 at 700 °C, respectively. The enhancement in electrical performance for anode-supported SOFC single cells could be mainly attributed to the increase of the ion transmission area of the anode/electrolyte interface and the increase of ionic conductivity of the dense, crack-free electrolyte layer.

2.9.3 Multilayer anodes development

Single layer Nickel/YSZ cermet anodes show high degradation during long term operation that can be ascribed to the agglomeration of Nickel particles (A.C. Müller et al. 1998). It could be shown that the degradation rate strongly depends on current density and fuel utilization. It is assumed that either ohmic losses across thin electrical contacts or polarization losses at the Three-Phase Boundary (TPB) locally increase the temperature and originate the agglomeration of the initial small nickel particles. Insufficient removal of water vapor results in Ni oxidation, which can lead to agglomeration (T. Weber, 1990).

A reasonable way to prevent degradation and increase performance could be a multilayer anode. The idea is shown in Figure 2.9.4 below.

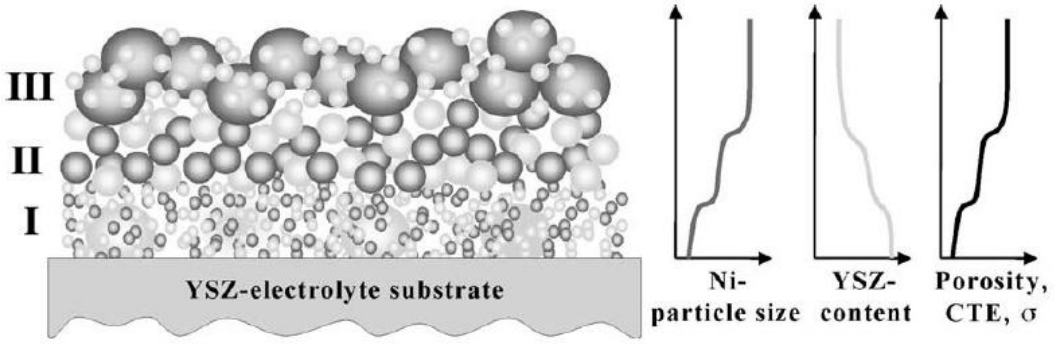

Figure 2.9.4 Illustration of a multilayer anode with gradients in composition and microstructure. As a consequence of the different composition of the diverse functional layers the physical properties (CTE, porosity, etc.) of the anode also vary. Source: Axel C. Müller et al. 2002.

Axel C. Müller, Dirk Herbstritt and Ellen Ivers- Tiffée (2002) investigated cermet (NiO–8YSZ) bulk samples with different composition, particle sizes and sintering temperature. The total porosities of the reduced and oxidized samples were determined geometrically. They also tested cells with a single layer anode made of different composition NiO-8YSZ cermets. This work is valuable to future researchers of multilayer anodes because it states the composition of the anode in various layers theoretically needed to obtain the best performance. The process of manufacturing such an anode will be difficult and the number of anode layers vs. performance boost is still an open question.

Cofired single cells investigated in the work (Axel C. Müller et al. 2002) are only the first step in the development of multilayer anodes. Therefore an increase in performance could be expected for the final multilayer anode with additional layers and a top layer with higher Ni content optimized for current collection.

2.9.4 Single chamber SOFCs with integrated current-collectors

For SOFCs the engineering problems, and therefore costs, are partly due to the processes and technologies required for sealing the cells at high temperatures. Single chamber solid oxide fuel cells (SC-SOFCs) with reaction selective electrodes offer the possibility to simplify SOFC designs because only one gas compartment is necessary. Both anode and cathode are exposed to the same mixture of fuel and oxidant. In such a system the driving force for the ionic current in the electrolyte is not due to the difference of oxygen partial pressures in the two sealed gas compartments. It is the selectivity of the two different electrodes for either the partial oxidation of methane (anode) or the reduction of oxygen

(cathode) that gives rise to the observed Open Circuit Voltage (OCV, [V]) (B.E. Buergler et al. 2005).

A scheme of such a SOFC system is shown in Figure 2.9.5 below.

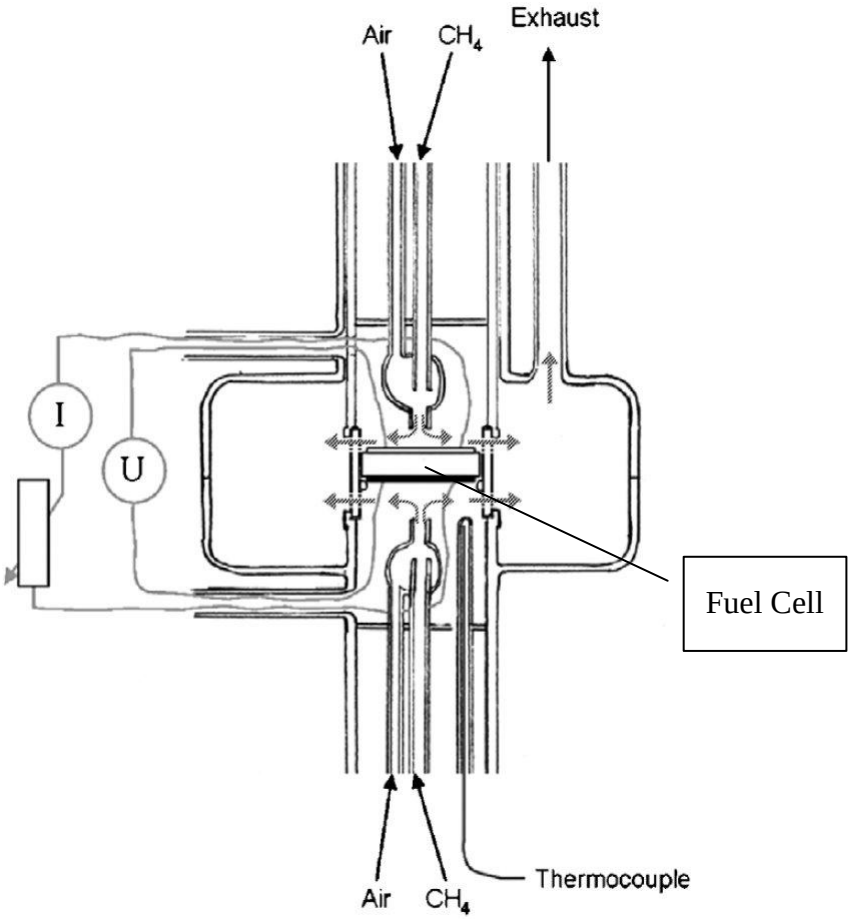

Figure 2.9.5 SC-SOFC measurement setup with mounted cell. The arrows indicate the gas mixture movement directions in the setup. Source: B.E. Buergler et al. 2005.

The authors claim that the performance of such a system is good because of the selective electrodes, especially the anode which has been specially modified by the addition of ceria supported Pd–catalyst (Pd–CeO_2) to the NiO–CGO powder prior to screen printing. The results of tests on the SC-SOFC are shown in Figure 2.9.6 below.

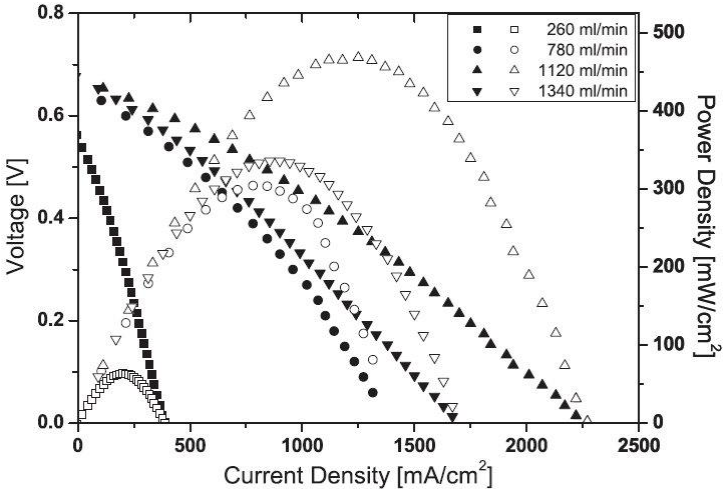

Figure 2.9.6 Voltage (closed symbols) and power density (open symbols) vs. current density of a SC-SOFC with 0,29 mm thick electrolyte at 600 °C for different air flows (260, 780, 1120 and 1340 ml/min) and a constant flow of 380 ml/min CH_4. Source: B.E. Buergler et al. 2005.

What can be easily noticed is the performance's strong dependency on the flow rate of the CH_4–Air mixture composition.

A very interesting comment on the SC-SOFC was published recently by I. Riess in the Journal of Power Sources (I. Riess, 2008). Riess gives an example of how the gas composition and flow are handled. Let the gas mixture consist of methane and air. The following limitations are imposed: (a) the fuel oxygen mixture is fuel rich with a ratio: CH_4:O_2 = 2:1, instead the one needed for full oxidation: 0.5:1; (b) the gas is split, half being directed towards the anode only and the other half towards the cathode only; (c) the flow rate is controlled to be high. The anode is not selective and in the gas flushing the anode full oxidation takes place. However, the limited supply of oxygen assures that only partial reforming occurs ($CH_4 + 1/2O_2 \rightarrow CO + 2H_2$). This is equivalent to supplying just fuel, of different nature (CO and H_2), to the anode side. The cathode is flushed with the gas mixture and it is assumed that the cathode is selective. Unfortunately, even the latter assumption is questionable since, if it were correct, the power output would not depend on the flow rate and fuel utilization could approach 25% instead of 1.5%, as mentioned before. This suggests that the cathode is not selective either (I. Riess, 2008).

The topic of the Single Chamber SOFCs is a recently developed branch of science and unfortunately we need to wait some time for proof that these cells are actually efficient and worth the world's attention.

2.9.5 Innovative ways of manufacturing SOFCs

The usual method of Solid Oxide Fuel Cells manufacturing is sintering the layers (for example anode, anode interlayer, electrolyte, cathode interlayer and cathode) in different temperatures (1000-1400 °C)

Gunter Schiller et al. (n.d.) proved a different way of SOFC manufacturing. Their invention is based on Vacuum Plasma Spray technology. This process is based on the generation of a plasma jet consisting of argon or argon with admixtures of H_2 and He, which are ionized by a high current arc discharge in a plasma torch. The powders to be sprayed are injected into the plasma where they are accelerated, melted and finally

projected onto a substrate. The coating is formed by the solidification and flattening of the particles at impact on the substrate. By operating the spray process in a chamber with reduced pressure, a long and laminar plasma jet with high velocity and reduced interaction with the surrounding cold gas is formed, resulting in improved spray conditions (Gunter Schiller et al. n.d.).

This technology is emerging because of the potential in fabricating large SOFC cells up to a square size of 20 x 20 cm^2. This cell has an area 8 times bigger than the SOFCs analyzed in this master thesis. Such cells are, I believe, the future of electricity generation both from fossil hydrocarbons and also from renewable fuels as bio-ethanol or hydrogen electrolyzed with clean electricity.

3 ENERGY RESEARCH CENTER OF NETHERLANDS (ECN), FUEL CELL LABORATORY IN PERUGIA (FCLAB) – INTERNATIONAL COOPERATION OVERVIEW AND CURRENT PROJECTS

3.1 Energy Research Center of Netherlands (ECN)

The Energy research Centre of the Netherlands (ECN) is the largest research centre in the Netherlands in the field of energy. At this moment ECN employs about 900 people. ECN is situated in the dunes near Petten, a village in the northern part of Holland. The research centre carries out research in the field of energy. With this work the researchers move between fundamental research at universities and the application of knowledge and technologies in practice. This work has a huge impact on daily life. For example, solar energy systems are placed on the roofs of houses and modern wind mills are spinning in the field by means of technology developed by ECN. With this the institute exerts an important function for the society of today and tomorrow (http://www.ecn.nl/en/corp/ accessed on 27th Jan. 2009).

The mission of ECN is to develop high-level knowledge and technology for a sustainable energy system and later transfer it to the real world market.

One of the ways by which this can be done is through cooperation with universities and research centers in different places in the world, such as FClab in Perugia.

3.2 Fuel Cell laboratory in Perugia, Italy (FClab)

3.2.1 Brief history of the University

The University of Perugia was founded in 1308 by the Pope Clemente V. The "Studium Generale" was one of the most famous Schools in Italy in the 14th century, where students could attend courses in law and medicine.

Between the 15th and the 17th century, courses of Science, Mathematics and Ancient Languages were also introduced.

The school of Engineering was founded in 1987: a new school in one of the oldest Italian Universities. Approximately 30000 students attend the University of Perugia and 3000 of them attend the School of Engineering.

3.2.2 The FCLab Group

The FCLab group is a dynamic and growing group, composed of two Professors, four researchers and several M. Sc. and Ph. D. students. The group is enlarged with cooperation with visiting researchers and professors from other Universities and research centers. The lab is a separate building located in the Engineering Faculty campus. A view of its interior is shown in Figure 3.2.1 below.

Figure 3.2.1 View on FClab interior.

3.2.3 FClab Activities and Projects

FClab Activities are divided into three main branches: numerical simulations, testing and system design. Most of the projects being realized in the lab contain all three of them. Usually the project starts with numerical simulations and system design. When these actions provide the calculations results and design of the system, the construction of the test benches begins and tests occur in the end.

Numerical simulations are concentrated on the development of numerical codes, simulation of cells, analyses and optimization of plants and also analyses of cost, environmental footprint and reliability.

The system design branch investigates balance of plant (BoP) design, alternative fuel usage options and integrated components numerical/experimental performance comparison.

Fuel Cell testing is the widest field of research in FClab. This branch of activity is developed for:

- Fuel Cells performance evaluation
- Fuel flexibility
- Pollutant effects assessment
- Durability Analysis
- Thermal Cycling
- Procedure harmonization and standardization

The challenge of this work was to bring back to life the Solid Oxide Single Cell test bench, which was disassembled and further tests could not be performed for a longer period. The lab needed detailed procedures for software set up, hardware configuration of the test bench and performing tests.

Also, because the FClab joined the FCTESTNET network (see paragraph 5.1 page 37), another goal of this work was to analyze FCTESTNET procedures and adapt them for our SOFC single cell test facility.

FClab in the past took part in different projects regarding Polymer Electrolyte Membrane Fuel Cells. Now it is concentrated on testing Solid Oxide Fuel Cells and Molten Carbonate Fuel Cells.

The projects being realized now are:

ECN – SOFC Single Cell (see Figure 3.2.2 below)

Figure 3.2.2 SOFC Single Cells test bench.

- Project partner: InDEC B.V., the Netherlands
- Sponsor: Internal Funds
- Objective: Characterization of electrolyte supported and anode supported single cells and investigation of their performance with different fuels and pollutants

This is the project I was engaged in. As I arrived the test rig was not ready to perform tests. We had to install the power supply, electronic load and new cables for them. Also the MFCs were not working correctly; one of them had to be substituted. The new software for data acquisition is still being developed, but its last beta version is an application written in NATIONAL INSTRUMENTS™ LabVIEW™ 8.6 environment and it is ready to use. It does not support all the functions that would make the work on the test rig easier, but at the moment it is working well enough to give proper results from tests.

During my stay in Perugia the test facilities for other projects were still in development.

ISOS – Investigation of Short Solid Oxide Stacks (see Figure 3.2.3 below)

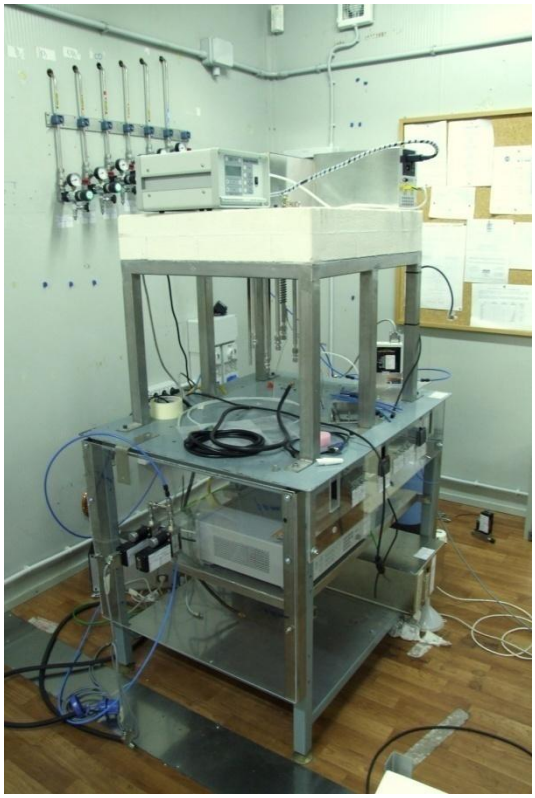

Figure 3.2.3 Short solid Oxide Stacks test bench.

- Project partner: FZJ Juelich, Germany
- Sponsor: Internal Funds
- Objective: Characterization of short SOFC stacks made of 4 planar single cells 10x10 cm, under different operating conditions and durability tests
- This project has just started and the facilities are under construction

CERSE – Molten Carbonate Fuel Cell (MCFC) single cell

- Project coordinator: ENEA
- Other partners: FCLab, Ansaldo Fuel Cells S.p.A.

- Sponsor: Italian Ministry of Education
- Objective: Competitive MCFC development
- This project has just started and the facilities are under construction

FISR 2003 – MCFC stack (see Figure 3.2.4 below)

Figure 3.2.4 MCFC stack test bench.

- Project coordinator: FCLab
- Other partners: Ansaldo Fuel Cells S.p.A., Centro Sviluppo Materiali SpA, ISRIM S.c.a.r.l
- Sponsor: Italian Ministry of Education
- Objective: Competitive MCFC development

3.2.4 International cooperations and main partners of FClab

FClab in Perugia widely cooperates with partners from different countries. This helps the lab to stay in touch with the newest science achievements and helps in financing projects. Key partners of FClab are listed in Table 3.2.1 on the next page.

Table 3.2.1 Partners of FClab.

Name of cooperator	Logo
ECN-InDEC-H.C. Starck	
ENEA Research Center	
Ansaldo Fuel Cells S.p.A.	
FZ Juelich	
HTCeramix	
MTU CFC Solutions	
SOFC POWER	
Merloni Group	
RES|The School for Renewable Energy Science	

The FClab in Perugia is a very modern undertaking that is able to perform tests on different fuel cells. The part I was working on (SOFC single cells testing) is the most developed project in the lab. It is possible now to perform different tests with hydrogen fuel on round planar SOFC cells of 80 mm diameter. Shortly it will be possible to investigate pollutant influence on the SOFC performance, stability and durability. Also, introducing different fuels is planned, as mentioned in the objectives of this work.

4 SINGLE STACK – DETAILS OF THE TEST FACILITY

4.1 How does the system work

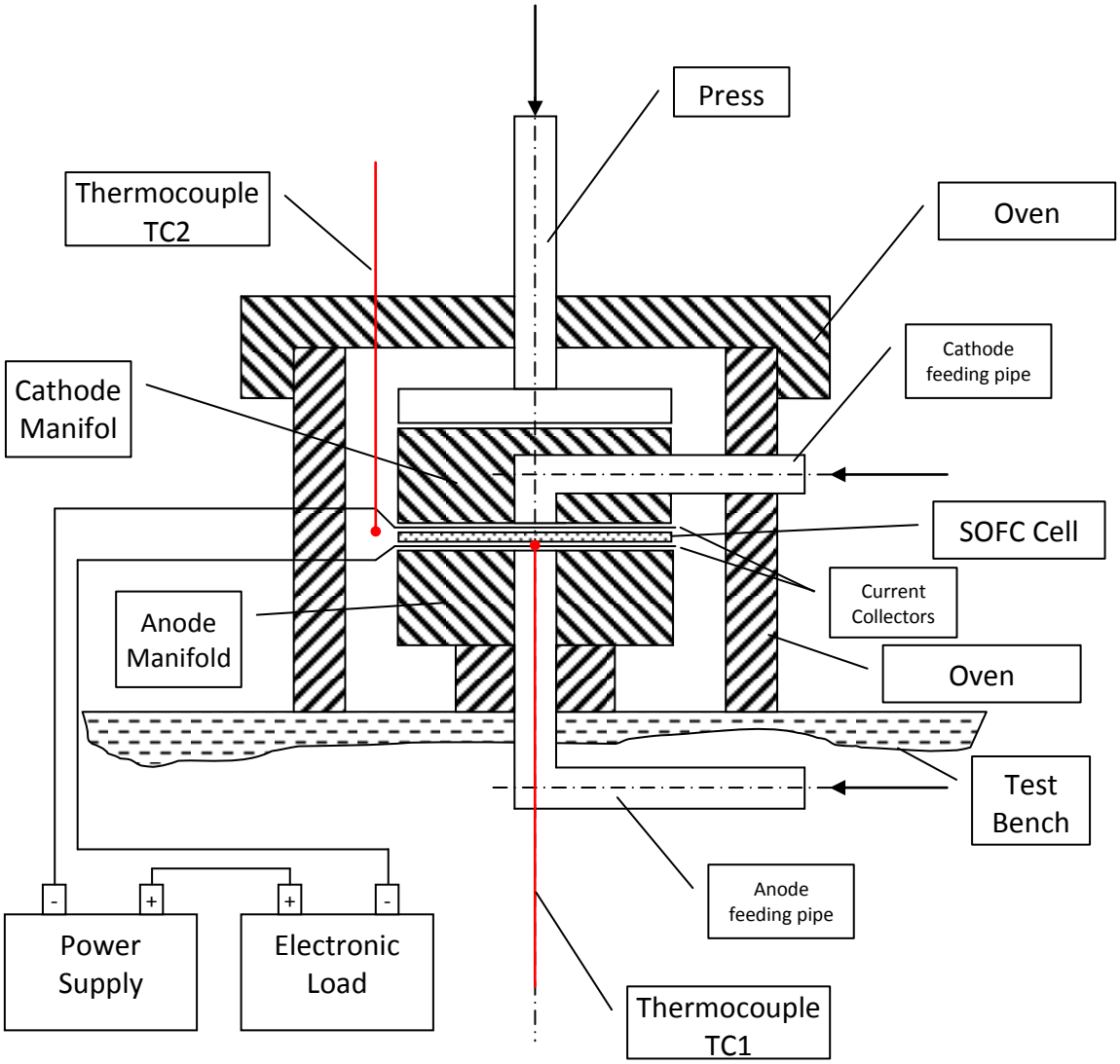

Figure 4.1.1 Scheme of the test rig.

The scheme of our test rig is shown in Figure 4.1.1 above. Red lines show the TCs location.

During the Fuel Cell performance test the system works as follows:

Each of the three gas pressures are set to 3 bars between the pressure regulators and MFCs. The PC manages gas flows through the MFCs and the electronic load. It also acquires data from the NI data acquisition unit (two temperatures and voltage).

Hydrogen gas flows through the MFC with a constant rate (controlled in real time by PC). On its way it passes the humidifier and is supplied to the anode manifold and further flows on the cell. Air is supplied without humidifying through the cathode manifold, using another MFC with a constant rate (also controlled in real time by the PC).

The temperature is maintained by the oven connected to the thermo regulator (programmed manually according to the lab procedure).

The cell is compressed by the pneumatic press and the weight of the cathode manifold, ceramic disc and cylinder in between.

The voltage of the cell is measured using the cables connected directly to the meshes of current collectors. The electronic load needs voltage (higher than that which is provided by the FC) to work, therefore the boost of 8V is supplied by the power supply.

All of these processes together provide the data to the computer that allows drawing the j-V curve, the power density curve and the temperature vs. time curve.

4.2 Main components list and components description

4.2.1 The tested Solid Oxide Fuel Cell

FClab in Perugia is testing SOFC cells provided by the ECN research center. These fuel cells were produced by InDEC B.V. belonging to H.C.Starck Ceramics.

The tests were performed with InDEC ASC2 (Anode Supported Cell type 2). Although it can be manufactured with different shapes (as these shown in Figure 4.2.1 below) we were testing only circular-shaped cells.

Figure 4.2.1 InDEC ASC2 Anode Supported Cell type 2 – different shapes. Source: InDEC B.V. ASC2 folder.

The lab was provided with basic data about the cell – materials and thicknesses of particular cell layers, typical geometrical qualification and a short notice about its features. Table 4.2.1 shows the basic cell layers description.

Table 4.2.1 Anode Supported Cell, type 2 (See Figure 4.2.2 below). Source: InDEC B.V. ASC2 folder.

SOFC layer	**Material**	**Thickness in µm**
Anode Support	Porous NiO/8YSZ	520 – 600
Anode	Porous NiO/8YSZ	5 – 10
Electrolyte	Dense 8YSZ	4 – 6
Blocking	Layer YDC	2 – 4
Cathode	Porous LSCF	20 – 30

Where:

- 8YSZ means 8 mol% Y_2O_3 doped ZrO_2
- YDC – Yttria doped Ceria
- LSCF – Lanthanum Strontium Cobalt Ferrite Oxide

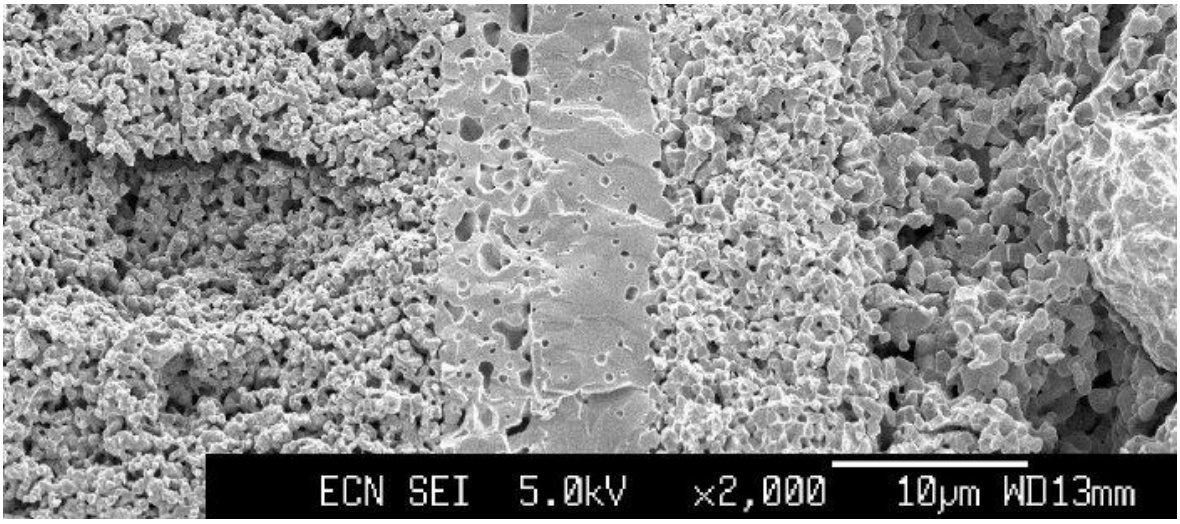

Figure 4.2.2 SEM micrograph of the cell cross-section (from the left: Cathode, Blocking Layer, Electrolyte, Anode, Anode Support). Source: InDEC B.V. ASC2 folder.

Table 4.2.2 Typical geometrical qualification. Source: InDEC B.V. ASC2 folder.

Parameter	**Typical Sizes in mm**
Maximum Size	200 × 200
Lateral Size Tolerance	± 0.1
Total cell thickness	0.55 – 0.63

Table 4.2.3 Diameters of the tested cell (See Figure 4.2.3 below)

Diameter	Diameter in mm
Outer diameter (anode diameter)	80
Cathode inner diameter	10
Cathode outer diameter	78

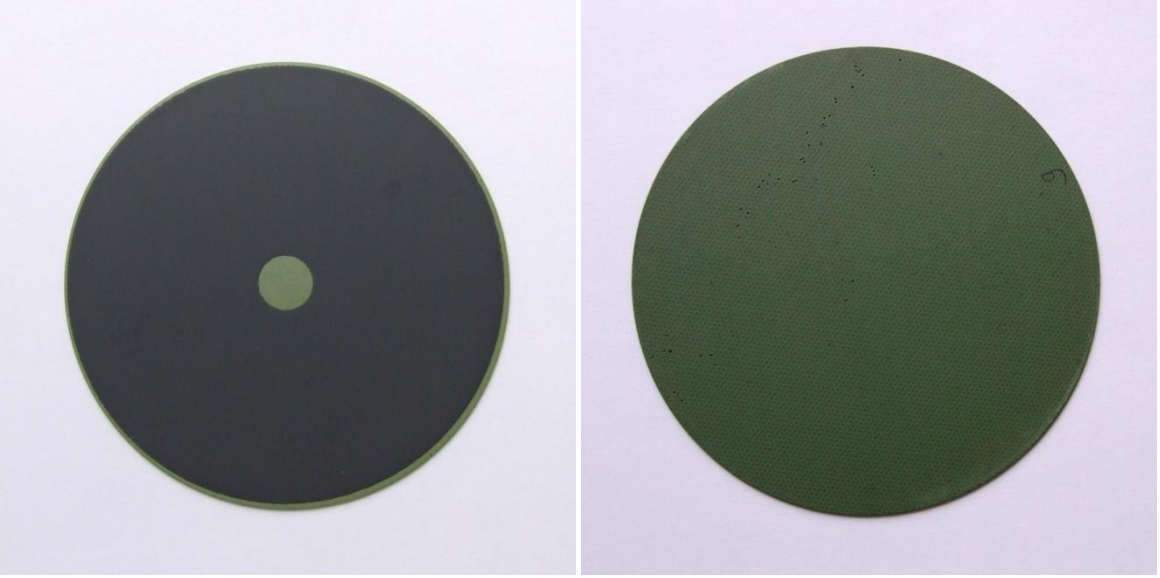

Figure 4.2.3 ASC2 cathode and anode before tests.

In addition the producer states that ASC2 is a SOFC cell suitable for intermediate temperature operation, 650 – 800 °C. The serial number of the tested cell was: **KS4X041015 – 7**.

4.2.2 Central system

- Fuel and Oxidant manifolds (see Figure 4.2.4 below)

  Manifolds were provided by the ECN research center in the Netherlands. They were made out of ceramic materials which can survive temperatures above 1000 °C.

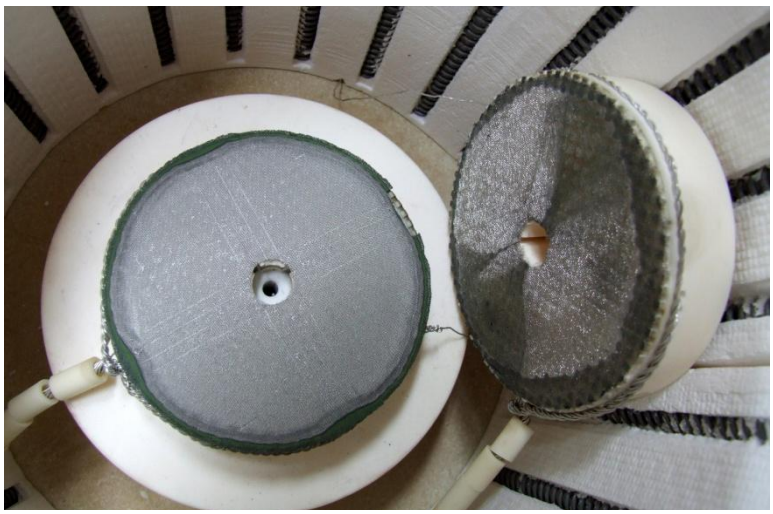

Figure 4.2.4 Anode (left) and cathode (right) manifolds.

- Three thermocouples

  Two of them connected to the NI data acquisition unit and one directly to the thermo regulator of the oven.

- Frame and plexi glass case with exhaust ventilation pipe

  Made of steel, aluminum and plexi glass.

4.2.3 Gas feed regulation equipment

- BROOKS Smart Mass Flow Controller (MFC) for hydrogen #47400003

  After the pressure regulator (see paragraph 4.2.8 page 36), hydrogen meets a triple connector on its way, leading it to two MFCs. There are two of them to increase accuracy of the measurement in the low flows range. The first MFC #47400003 manages the flows of hydrogen up to 30 Nl/h.

- BROOKS Smart Second MFC for hydrogen #03308005

  Has the same function as MFC mentioned above, but its range is 0-50 Nl/h what makes it less accurate for the lower flows range.

- BROOKS Smart MFC for nitrogen #47400004

  Nitrogen goes through a MFC #47400004 in range 0-80 Nl/h.

- BROOKS Smart MFC for air #03308004

  Air supply is managed by a MFC #03308004 which allows flows in range 0-130 Nl/h.

4.2.4 Electronic devices

- DC power supply Agilent Technologies N5763A (see Figure 4.2.5 below)

Figure 4.2.5 DC power supply Agilent Technologies N5763A.

This device is used to increase the voltage by 8V and it follows the load in the circuit.

- Electronic load Agilent N3301A (see Figure 4.2.6 below)

Figure 4.2.6 Electronic load Agilent N3301A.

Electronic load can be maintained directly from the PC.

- Electric furnace system (see Figure 4.2.7 and Figure 4.2.8 below)

Figure 4.2.7 Thermo regulator – control panel of the electric furnace.

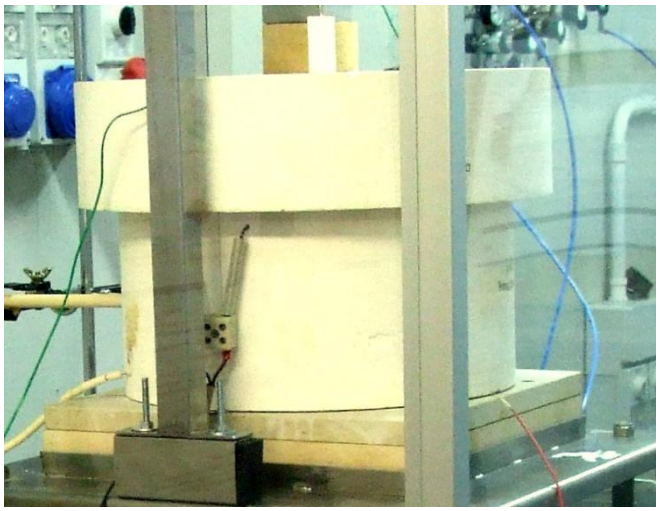

Figure 4.2.8 Electric furnace during operation.

This system contains the oven chamber and the thermo regulator device connected to each other with electric cables. The thermo regulator has its own thermocouple of the same type as mentioned before. The operator can set the oven temperature and the heating speed. The heating speed in our system was set to 27 °C/h. The system was usually heated to 800 °C. And then higher temperatures where set higher if needed for specific tests.

- National Instruments (NI) data acquisition unit, connected to a PC

  This device gains:

  - Two temperatures from the two thermocouples (TCs), one used to check the temperature of the oven and the other to see the temperature of the cell, installed on the anode side.
  - Cell voltage.

4.2.5 Humidifying unit for humidification of fuel gas feed (see Figure 4.2.9 below)

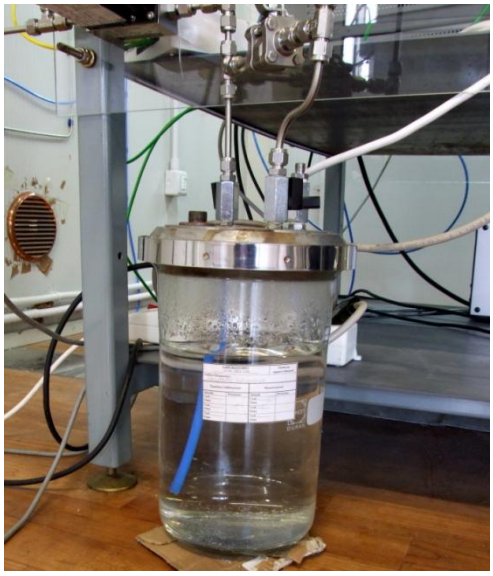

Figure 4.2.9 Humidifying unit.

A container filled with purified water. The hydrogen and nitrogen go through it to be humidified. The humidifier can be bypassed so that the gases will be dry.

4.2.6 Pneumatic press (see Figure 4.2.10 below)

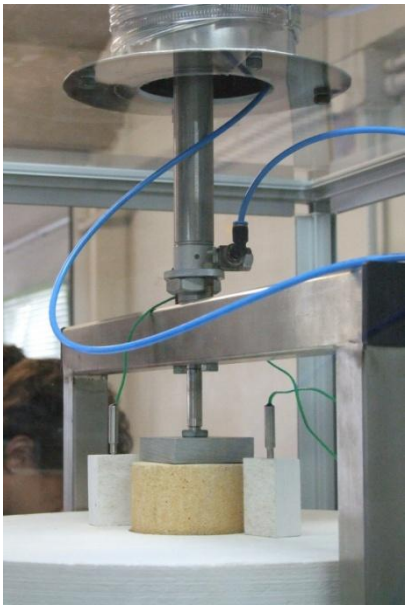

Figure 4.2.10 Pneumatic press piston.

A pneumatic press is used to increase the cell pressure and lets the manifolds touch the cell more tightly.

4.2.7 PC including

- National Instruments Data Acquisition card (hardware)

  Which allows the two temperatures from TCs and voltage to be acquired by the PC.

- Control System software (see Figure 4.2.11 below)
- Smart DDE software

  Software used for managing com ports and MFCs

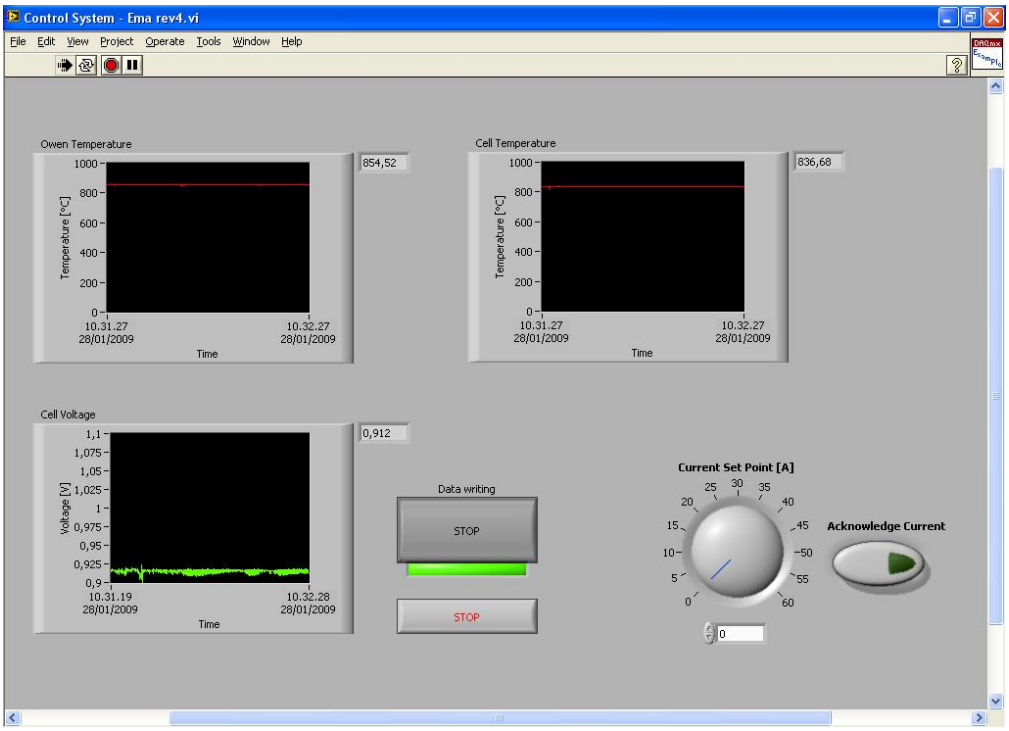

Figure 4.2.11 Control System software.

Software used for load control and data acquisition. In the upper left corner is the oven temperature indication (thermocouple placed in the oven). The history of the last minute is visible. In the upper right corner is the indication of the thermocouple placed in the inlet to the anode manifold. In the left bottom is the cell voltage indication graph. In the bottom center are two buttons responsible for starting/stopping data writing and stopping data acquisition. On the bottom right the current can be set either by typing in the number of amps or by using the jog and clicking the button on the bottom right

- Sistema di Controllo Laboratorio software (see Figure 4.2.12 below)

  Software used for managing Mass Flow Controllers. In Figure 4.2.12 below the first MFC is configured and ready to use. The value of Nl/h is entered and the actual flow and measurement error can be seen. Maximum 8 MFCs could be managed at once by this software.

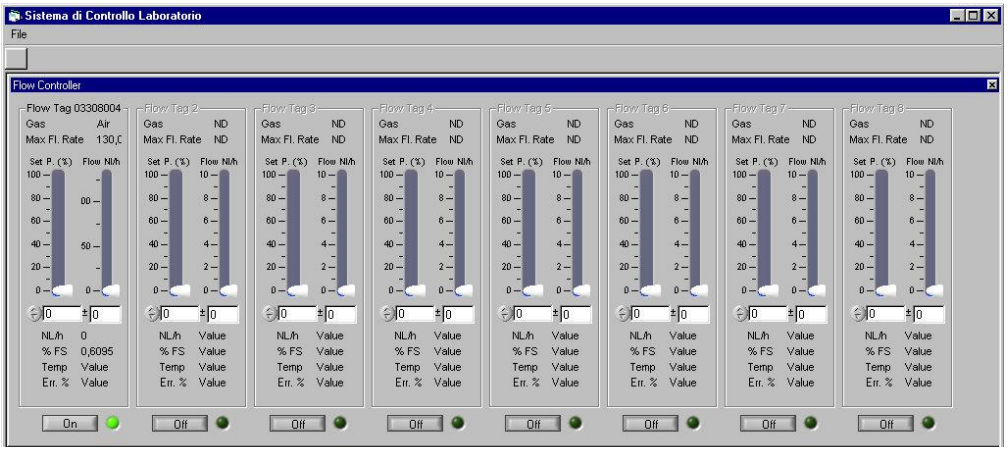

Figure 4.2.12 Sistema di Controllo Laboratorio software.

4.2.8 Hydrogen, Nitrogen and Air storage and supply systems

All gas storage and supply systems are located outside the laboratory in the fresh air, behind a concrete double layer wall of 2 x 30 (60) mm thickness. Each type of gas has its own separate space. The twelve 200-bar container vertical bundle is a set of twelve 200-bar standard 10 Nm^3 gas storage containers connected together, acting as a one 120 Nm^3 gas storage tank. The containers are connected to one manometer and valve, which lets the gas enter the laboratory through special holes in the wall. Inside the laboratory there is a valve for each gas as well as a pressure regulator.

Hydrogen storage and supply system contains of:

- Twelve 200-bar containers vertical bundle
- One reserve H_2 storage 200-bar container
- Necessary valves and pipes, including automatic switch to the reserve container
- Pressure regulator located inside the lab

Nitrogen storage and supply system contains of:

- Twelve 200-bar containers vertical bundle
- One reserve N_2 storage 200-bar container
- Necessary valves and pipes
- Pressure regulator located inside the lab

Air supply system contains of:

- Compressor
- Container for compressed air storage
- Reserve compressed air storage in twelve 200-bar containers vertical bundle

5 TESTS

Introduction:

Having a Fuel Cell lab professionally equipped and cooperating with the best in the world, all that is needed to begin the real science is to start performing tests of the Solid Oxide Fuel Cells. At the beginning a common way of testing SOFCs had to be chosen. It was decided to use the FCTESTNET procedures (paragraph 5.1), which probably will become a standard in Europe, and possibly worldwide. Later calculations had to be made regarding the hydrogen and nitrogen consumption for particular tests and how long these tests would take. The spreadsheet was extended on calculations of other possible gases (methane, carbon monoxide carbon dioxide) and pollutants (mixtures of hydrogen with hydrogen sulphide gases). These gases are used in SOFC tests to simulate the cell's performance on different fuels and the influence of pollutants such as sulphur on the cell's performance. The spreadsheet will be called Single SOFC Test Bench Model (paragraph 5.2). The cell temperature also has to be estimated somehow. The model for this estimation has been created (paragraph 5.3). To compare the results of the experiments with theory the Reversible Voltage calculations have been performed (paragraph 5.4). To perform any experiment in a high quality lab, the detailed procedures are needed and have been prepared (paragraph 5.5).

5.1 The FCTESTNET procedures

The Fuel Cell laboratory in Perugia has its own procedures for the test facility operation (start-up, cool-down, software and hardware setup) but the cell performance tests are being done according to Fuel Cell Systems Testing, Safety & Quality Assurance standards (FCTES^{QA}). As can be found on its webpage (http://fctesqa.jrc.ec.europa.eu/), this organization is a Specific Targeted Research Project (STREP) co-financed by the European Commission within the Sixth framework Program.

The main aim of FCTES^{QA} is to address the aspects of pre-normative research, benchmarking, and validation through round robin testing of harmonized, industry-wide test protocols and testing methodologies for fuel cells. This activity will provide support for the essential pre-normative research efforts towards standardization, thereby contributing to the early and market-oriented development of specifications and pre-standards.

For the first time, the internationally agreed harmonized test procedures applicable to fuel cells, stacks, and systems, which were the output of the FCTES^{QA} predecessor project, namely, the "Fuel Cell Testing and Standardization Network" (FCTESTNET), will be validated through experimental campaigns. Test protocols will undergo benchmarking and round robin testing in different laboratories. FCTES^{QA} results will be discussed, debated and agreed in co-operative progress meetings and dedicated international workshops under the International Partnership for the hydrogen Economy (IPHE) auspices. In addressing the above-mentioned issues an international consortium from EU and IPHE members has been established.

The present project will help to bridge the gap between individual and independent management decision-making within companies and research groups and the outcome and experience of different research activities worldwide with harmonized, validated, and benchmarked procedures following accepted international quality practices (http://fctesqa.jrc.ec.europa.eu/).

The following test procedures for solid oxide single cells are available on FCTESTNET:

- Cell Polarisation - H_2 (Hydrogen) (see Appendix D)
- Cell Polarisation - IR-CH_4 (Internally Reformed Methane)
- Cell Polarisation - ESR-CH_4&Diesel (Externally Reformed Methane and Diesel)
- Cell Polarisation - POX&ATR-diesel (Reformed with Partial Oxidation reformer and Auto Thermal Reformer Diesel)
- Cell Endurance - H_2
- Cell Endurance - IR-CH_4
- Cell Endurance - ESR-CH_4&Diesel
- Cell Endurance - POX&ATR - Diesel
- Cell Performance&Endurance - H_2
- Cell Performance&Endurance - IR-CH_4
- Cell Performance&Endurance - ESR-CH_4&Diesel
- Cell Performance&Endurance - POX&ATR - Diesel
- Cell Sulphur tolerance
- Cell Thermal cycling H_2

FC Laboratory in Perugia is able to perform some of these tests already. The goal is to be able to perform all of them on some cells to show their performance on different fuels in different temperatures and to investigate the influence of a pollutant – sulphur – on cell's performance and durability.

The point which is important in the FCTESTNET tests is that to check the cell performance on diesel fuel it is not required to have a diesel reformer, which would be an External Steam Reformer or a Partial Oxidation reactor with Auto Thermal Reformer. There are anode gas compositions given to simulate different fuels. The only doubtful thing is no sulphur in diesel fuel in those tests, but it can be grounded in the presence of an additional sulphur tolerance test. A sample FCTESTNET procedure can be found in the Appendix D)

5.2 Single SOFC Test Bench Model (part of this work)

The Single SOFC Test Bench Model is a crucial part of this work. It has been prepared on the basis of FCTESTNET procedures, FClab procedures and the laboratory experience.

It is a general model of the laboratory included in one spreadsheet. It allows forecasting the time needed for specific tests and gases consumption. Cost evaluation is also included based on the recent (2008) prices of gases, including container rent and delivery. In the model each type of test has its own worksheet.

The user inputs the following data:

- How many different tests are to be performed.
- How many different temperatures are to be investigated during polarization tests.

As the outcome of the spreadsheet the user obtains the number of days needed to finish the tests and the costs of operation. The user uses only the "Summary" worksheet; other worksheets should not be modified. The interface of the summary tab is user-friendly and user-proof.

The Summary tab is shown in Figure 5.2.1 on page 40.

Within this work all the worksheets of the spreadsheet have been prepared. The list of worksheets included in the model is as follows:

- Summary – in this worksheet the user inputs the number of tests that he wants to evaluate the gas consumption, cost and required time for
- Cell data, variables&constants – here are the cell area and safety coefficients for time and gas consumption
- Costs – worksheet with prices of gases
- Start-up – worksheet evaluating the start-up procedure gas consumption and time
- Stabilization
- Cool-down

The rest of worksheets are the FCTESTNET procedures transformed to a spreadsheet. Additionally there is a "Sulphur system optimization" worksheet designed to help introducing sulphur tolerance test equipment to the existing test facility

One start-up and cool-down cycle only takes as much as 5 days and 7 hours, not taking into account the safety coefficient for time, which is 1,5. It is, however, possible to do many tests with only one start-up and cool-down, which will shorten the testing time and eliminate risks caused by human error during the start-up or cool-down period.

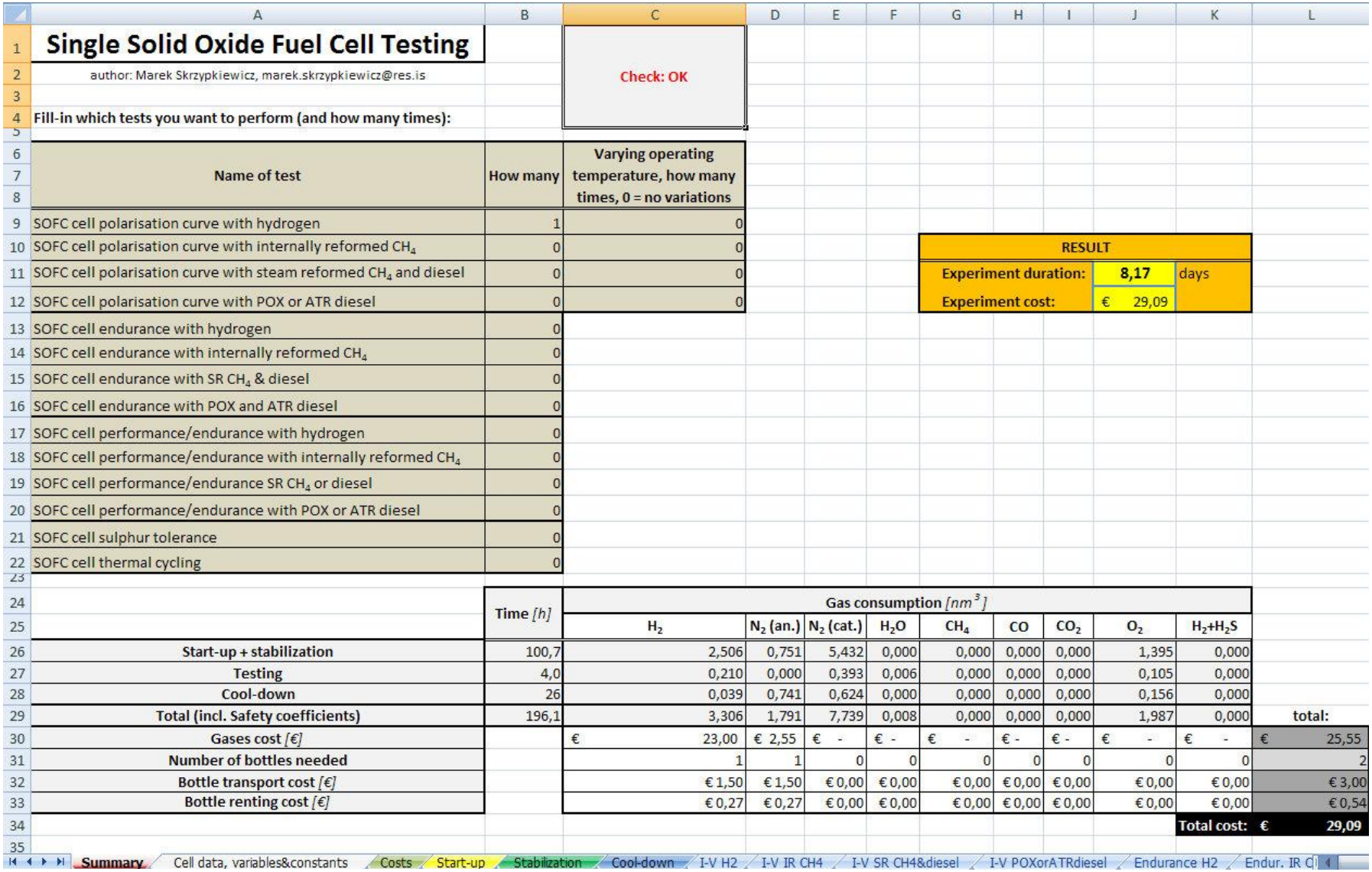

Single Solid Oxide Fuel Cell Testing

author: Marek Skrzypkiewicz, marek.skrzypkiewicz@res.is

Check: OK

Fill-in which tests you want to perform (and how many times):

Name of test	How many	Varying operating temperature, how many times, 0 = no variations
SOFC cell polarisation curve with hydrogen	1	0
SOFC cell polarisation curve with internally reformed CH_4	0	0
SOFC cell polarisation curve with steam reformed CH_4 and diesel	0	0
SOFC cell polarisation curve with POX or ATR diesel	0	0
SOFC cell endurance with hydrogen	0	
SOFC cell endurance with internally reformed CH_4	0	
SOFC cell endurance with SR CH_4 & diesel	0	
SOFC cell endurance with POX and ATR diesel	0	
SOFC cell performance/endurance with hydrogen	0	
SOFC cell performance/endurance with internally reformed CH_4	0	
SOFC cell performance/endurance SR CH_4 or diesel	0	
SOFC cell performance/endurance with POX or ATR diesel	0	
SOFC cell sulphur tolerance	0	
SOFC cell thermal cycling	0	

RESULT		
Experiment duration:	8,17	days
Experiment cost:	€ 29,09	

	Time *[h]*	Gas consumption *[nm^3]*									
		H_2	N_2 (an.)	N_2 (cat.)	H_2O	CH_4	CO	CO_2	O_2	H_2+H_2S	
Start-up + stabilization	100,7	2,506	0,751	5,432	0,000	0,000	0,000	0,000	1,395	0,000	
Testing	4,0	0,210	0,000	0,393	0,006	0,000	0,000	0,000	0,105	0,000	
Cool-down	26	0,039	0,741	0,624	0,000	0,000	0,000	0,000	0,156	0,000	
Total (incl. Safety coefficients)	196,1	3,306	1,791	7,739	0,008	0,000	0,000	0,000	1,987	0,000	total:
Gases cost *[€]*		€ 23,00	€ 2,55	€ -	€ -	€ -	€ -	€ -	€ -	€ -	€ 25,55
Number of bottles needed		1	1	0	0	0	0	0	0	0	2
Bottle transport cost *[€]*		€ 1,50	€ 1,50	€ 0,00	€ 0,00	€ 0,00	€ 0,00	€ 0,00	€ 0,00	€ 0,00	€ 3,00
Bottle renting cost *[€]*		€ 0,27	€ 0,27	€ 0,00	€ 0,00	€ 0,00	€ 0,00	€ 0,00	€ 0,00	€ 0,00	€ 0,54
										Total cost:	€ 29,09

Summary | Cell data, variables&constants | Costs | Start-up | Stabilization | Cool-down | I-V H2 | I-V IR CH4 | I-V SR CH4&diesel | I-V POXorATRdiesel | Endurance H2 | Endur. IR C

Figure 5.2.1 Single SOFC Test Bench Model, done in Microsoft Excel®.

The development of the model allowed seeing how long each part of the test takes. It can be planned when the crew has to be present in the lab to do some actions, and when the test facility works in constant conditions. In this way we can plan the tests to have a day off on Sunday, for example.

Also, as the objective of this thesis says, this spreadsheet was used for designing the pollutant supply to the system. The pollutant is the hydrogen sulphide (100 ppm) – hydrogen mixture. This is the highest concentration of H_2S that can be supplied with only one additional Mass Flow Controller without losing accuracy. With the system designed according to this spreadsheet it is possible to perform all sulphur tolerance tests designed by FCTESTNET.

5.3 Average Cell Temperature evaluation model

A very important component in presenting the results is the estimation of the Average Cell Temperature (ACT), which was calculated from the following formula:

$$T_{cell,average} = \frac{\int_{r_{cathode,min}}^{r_{cathode,max}} r\,T(r)\,dr}{\int_{r_{cathode,min}}^{r_{cathode,max}} r\,dr}$$

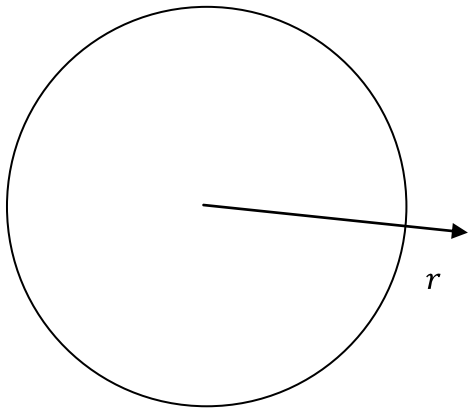

Figure 5.3.1 Coordination system for average cell temperature evaluation.

Where:

$$T(r) = \left(\frac{T_{cell,middle} - T_{oven}}{r_{cell,max}}\right) r + T_{cell,middle}$$

$r_{cathode,min}$ - inner radius of the cathode = 5 mm

$r_{cathode,max}$ - outer radius of the cathode = 39 mm

$r_{cell,max}$ - outer radius of the cell = 40 mm

$T_{cell,average}$ - average cell temperature

$T_{cell,middle}$ - middle cell temperature, provided by TC in the anode manifold

T_{oven} - oven temperature, provided by the TC in the oven space

Substituting $T(r)$ to $T_{cell,average}$ the final formula can be obtained:

$$T_{cell,average} = \frac{\int_{r_{cathode,min}}^{r_{cathode,max}} r \left[\left(\frac{T_{cell,middle} - T_{oven}}{r_{cell,max}}\right) r + T_{cell,middle}\right] dr}{\int_{r_{cathode,min}}^{r_{cathode,max}} r \, dr}$$

Substituting constants:

$$T_{cell,average} = \frac{\int_{5\ mm}^{39\ mm} r \left[\left(\frac{T_{cell,middle} - T_{oven}}{40\ mm}\right) r + T_{cell,middle}\right] dr}{\int_{5\ mm}^{39\ mm} r \, dr}$$

These calculations were done by the Temperature evaluation spreadsheet, see Figure 5.3.2 below.

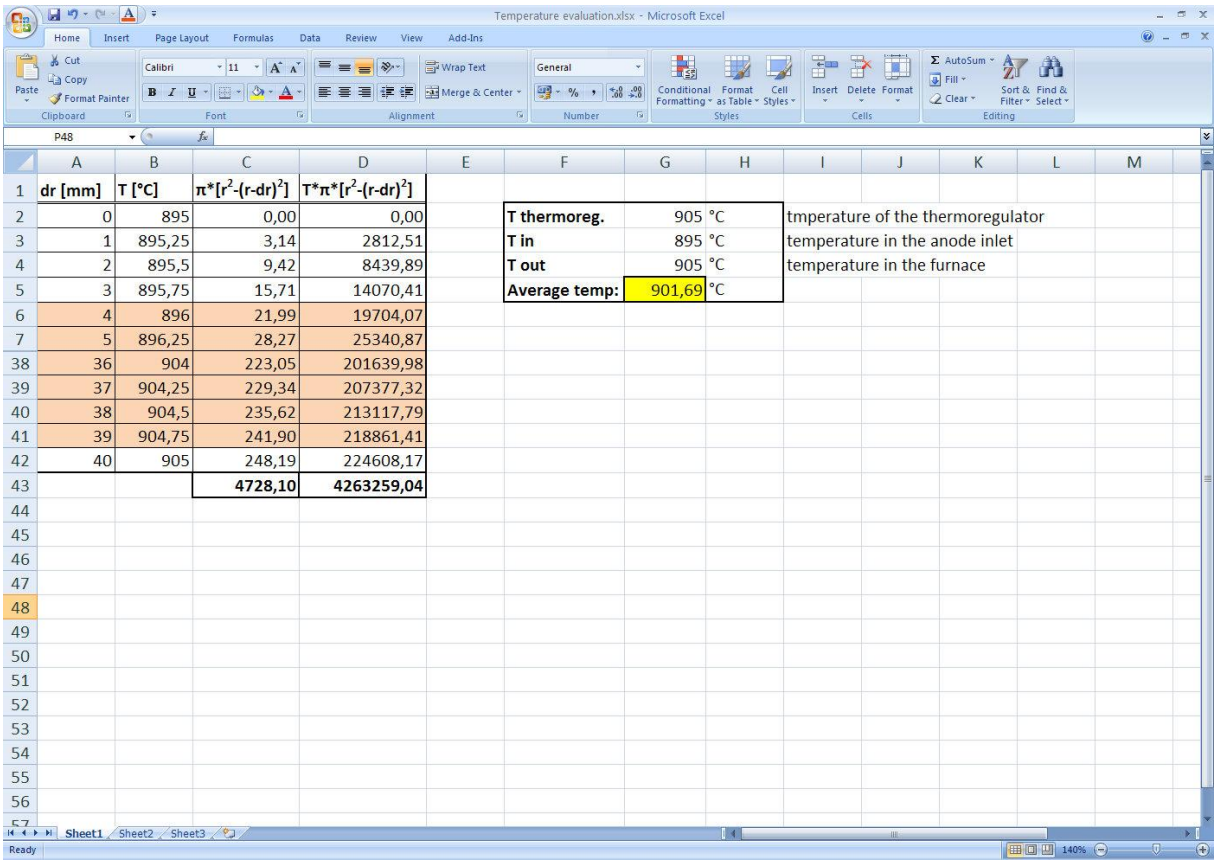

	A	B	C	D
1	dr [mm]	T [°C]	π*[r²-(r-dr)²]	T*π*[r²-(r-dr)²]
2	0	895	0,00	0,00
3	1	895,25	3,14	2812,51
4	2	895,5	9,42	8439,89
5	3	895,75	15,71	14070,41
6	4	896	21,99	19704,07
7	5	896,25	28,27	25340,87
38	36	904	223,05	201639,98
39	37	904,25	229,34	207377,32
40	38	904,5	235,62	213117,79
41	39	904,75	241,90	218861,41
42	40	905	248,19	224608,17
43			4728,10	4263259,04

T thermoreg.	905	°C	tmperature of the thermoregulator
T in	895	°C	temperature in the anode inlet
T out	905	°C	temperature in the furnace
Average temp:	901,69	°C	

Figure 5.3.2 Temperature evaluation spreadsheet prepared in Microsoft Excel®.

5.4 Reversible voltage calculations

Reversible voltage (E_T) depends on the cell operating temperature. It is described by the following equation (O'Hayre et al. 2006, p.43):

$$E_T = E^0 + \frac{\Delta \hat{s}}{nF}(T - T_0)$$

$\Delta \hat{s}_{rxn} = -44{,}43\ J/(mol \times K)$ for H_2O vapor as product.

$E^0 = 1{,}23V$

$T_0 = 298\ K$

$$E_T = 1{,}23\ V + \frac{-44{,}43\ J/(mol \times K)}{\left(\frac{2\ mol\ e^-}{mol\ reactant}\right) \times (96400\ C/mol)}(T - 298\ K)$$

$E_T(T = 700°C) = 1{,}074\ V$

$E_T(T = 750°C) = 1{,}063\ V$

$E_T(T = 800°C) = 1{,}051\ V$

$E_T(T = 850°C) = 1{,}04\ V$

$E_T(T = 900°C) = 1{,}028\ V$

These are the values that would occur in the no load (OCV) conditions in case of no other losses. For the comparison of theoretical values with the experiment results see paragraph 6.8.2 (beginning on page 54).

5.5 Description of the procedures used in FC Laboratory in Perugia

5.5.1 Start-up procedure

Before a test in the Fuel Cell Laboratory starts, the test rig is prepared and then the start-up procedure is performed.

In most cases start-up begins with installing the cell in its place of operation. To do it, the anode (bottom) ceramic manifold has to be installed first and connected to the fuel feeding pipe. The thermocouple is placed inside it and has to be installed about 1 mm from the bottom of the cell.

The cell is then put on the anode manifold concentrically; the anode lies on the anode manifold and the cathode faces up.

Once the cell is in place the cathode manifold needs to be installed, the cables checked – two thin cables go to the Data Acquisition Box, and two thick cables in ceramic covering go out of the oven and are connected in one circuit with the electronic load and power supply units (see Figure 4.2.5 page 32 and Figure 4.2.6 page 32). A heavy (~900 g) ceramic disc is placed on the cathode manifold. Then the oven is closed both from the side (if it was opened) and from the top; the cathode feeding ceramic pipe should not be connected yet (although it must be checked if everything is in the right position to install this pipe later).

After closing the cover another heavy cylinder (working both as ~1 kg weight to compress the cell and tappet for the pneumatic press) is placed vertically inside the aperture in the oven cover in the top. Then the oven wires are connected to the thermo regulator using two ceramic cube-connectors.

The press frame is mounted on the test rig after that; four bolts M6, 100 mm are used.

The test rig is ready for applying the weight (mechanic load) with the pneumatic press. It is done by setting the press pressure on the press control panel to 0,5 bar for 4,5 kg or to 1,8 bar for 11 kg weight. Initially the system is set for 4,5 kg of mechanic load, but it will be changed to 11 kg after heating up.

Later the ceramic cathode feeding pipe is installed carefully through an aperture in the oven. This part is extremely fragile. It should be screwed in carefully and rotated counterclockwise by 60 °. This way it is tight enough for heating up the flow of air, which is 30 Nl/h. Then the plastic air pipe should be connected to the ceramic feeding pipe with a plastic connector.

Screwing the ceramic pipe into the manifold more tightly can be done after heating-up and increasing the weight on the cell to 11 kg.

The gas feeds are set as follows: anode – H_2 = 1,5 Nl/h and N_2 = 28,5 Nl/h, cathode – Air = 30 Nl/h. Leak tightness must be checked on the anode and cathode feeding pipes.

The oven is launched to heat up the cell and manifolds to 800 °C with a ramp of 30 °C/h. For safety's sake it is now set to an effective heating rate of 27 °C/h.

When the temperature reaches 800 °C, which takes roughly 30 hours, the weight on the cell is increased to 11 kg, the cathode feeding pipe screwed in securely but stronger than before. The leakage of air should be checked on the plastic connector of the plastic air pipe with the ceramic cathode feeding pipe.

Then the reduction of the anode occurs by substituting N_2 from the anode gas feed with H_2. It is started from an H_2:N_2 proportion equal to 1,5:28,5 Nl/h and must be increased according to laboratory procedure. After 45 min the H_2:N_2 proportion is 30:0 Nl/h. This means that the anode is fed with only 30 Nl/h of Hydrogen.

The gas feed is then set as follows: anode – H_2 = 24 Nl/h, cathode – Air = 30 Nl/h.

If the Average Cell Temperature (see paragraph 5.3 page 41) is stabilized at 800 °C the j-V curve should be taken up to 50 A but the cell voltage cannot drop below 400 mV. After taking the last point of the j-V curve, the load is decreased to 16 A or less if the cell voltage is lower than 400 mV. This 16 A load should act on the cell for 48 hours. After this period the second j-V curve is taken in the same way as before.

5.5.2 Test procedure

Now the start-up procedure is completed and the tests can be performed.

This is the moment when the actual testing starts. In our case we did the polarization tests of the ASC2 cell (produced by InDEC B.V., see chapter 4.2.1 page 28) at different temperatures (800, 750, 700, 850, 900 °C).

The gas feed is set as follows: anode – H_2 = 49,24 Nl/h, cathode – Air = 117 Nl/h but because of the software issue we only could work on flows lowered by 14,5%: H_2 = 42 Nl/h, cathode – Air = 100 Nl/h. This increases the fuel utilization and should reduce the performance only slightly in the high current density region.

The polarization curve is taken starting from OCV up to the moment the voltage drops under 0,6 V or the current density reaches 1,25 A/cm^2. On each step the current demand is increased by 50 mA/cm^2, which in our case (cell area 47 cm^2) is equal to 2,35 A/step. One step takes 180 seconds, the voltage reading should occur just before increasing the current.

Once the maximum current density of 1,25 A/cm^2 or the limiting cell voltage of 0,6 V has been achieved the measurement is stopped and we start to go back with the measurements with 2,35 A/step. In this way we obtain two curves – one is called "up" and the other one is called "down". The cell temperature is monitored when taking all measurements.

After performing the polarization tests at the first temperature we set the thermo regulator for the next temperature (i.e. 750 °C) with the same ramp of 27 °C/h. When the cell reaches the temperature, it has to be stabilized according to FCTESTNET procedure. The stabilization of the cell occurs during the galvanostatic operation of the cell for a minimum of 4 hours, at a current density of 0,3 A/cm^2, which in our case is the load of 14,1 A.

5.5.3 Cool-down procedure

After all the tests the cool-down procedure occurs. This procedure starts with leaving the cell at OCV, changing gas composition to anode – H_2 = 1,5 Nl/h and N_2 = 28,5 Nl/h, cathode – Air = 30 Nl/h. Now the cathode feeding pipe should be rotated counterclockwise by 60 °. Then the thermo regulator must be set for the ambient temperature (i.e. 20 °C) with the same ramp as for heating (27 °C/h). After the ambient temperature is reached, the gas flows can be stopped and all devices of the test facility can be turned off.

6 RESULTS

The tests have been performed on the ECN test bench. The tested cell was InDEC ASC2 planar Solid Oxide Fuel Cell of diameter 80 mm (see paragraph 4.2.1 page 28).

During the whole start-up – five tests – cool-down procedure eleven j-V curves and eleven power density curves were obtained. The first two are during the start-up and they are not a comprehensive source of the cell performance information because of low gas flows. For each temperature we do two j-V curves, first with the load going up and the second with the load going down. The same is done with the power density curves, which are actually based on the same data as the j-V curves.

All the measurements were done in the lab with air condition set to 23 °C and ambient pressure oscillating around 1 atmosphere.

6.1 Start-up results:

Table 6.1.1 Gas feed parameters.

Gas type (MFC number)	**Flow rate Nl/h**
Air for cathode (03308004)	60
N_2 for anode (47400004)	0
H_2 for anode (47400003)	24 (Humidified at STP)
H_2 for anode (03308005)	0

Table 6.1.2 Test-rig parameters at test start.

Parameter	**Value in °C**
Cell Temp. (TC in the middle of the cathode)	792
Furnace Temp. (TC located in the Furnace space)	805
Average Cell Temperature	800,7

Results are presented on a graph (Figure 6.1.1 below). The tables with measurement results are included in Appendix B.

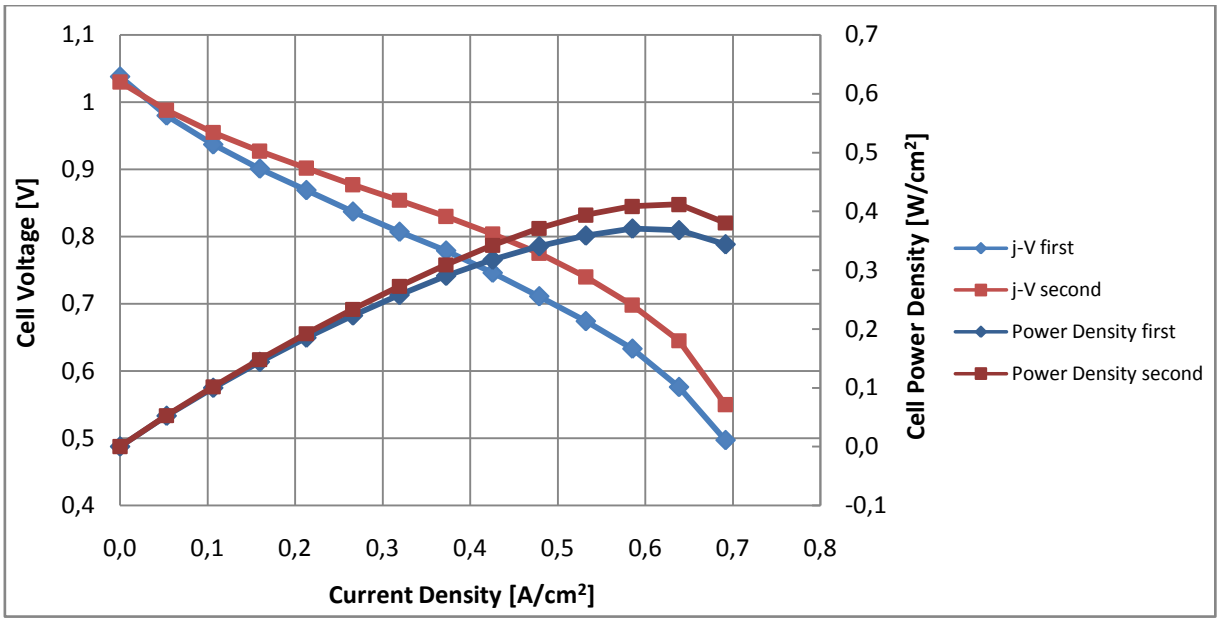

Figure 6.1.1 j-V and Power Density curves during start-up (24 Nl/h of H_2; 60 Nl/h of Air, Cell temperature 800 °C).

The start-up procedure was performed correctly. The result after 48 hours of stabilization at 16A gives better result. This is a natural behavior. Stabilization of the cell increases its performance.

6.2 Test no. 1 (Cell temperature 800 °C)

Table 6.2.1 Gas feed parameters.

Gas type (MFC number)	**Flow rate Nl/h**
Air for cathode (03308004)	100
N_2 for anode (47400004)	0
H_2 for anode (47400003)	42 (Humidified at STP)
H_2 for anode (03308005)	0

Table 6.2.2 Test-rig parameters at test start.

Parameter	**Value in °C**
Cell Temp. (TC in the middle of the cathode)	787
Furnace Temp. (TC located in the Furnace space)	806
Average Cell Temperature	799,7

The results are presented on a graph (Figure 6.2.1 below). The tables with measurement results are included in the Appendix B.

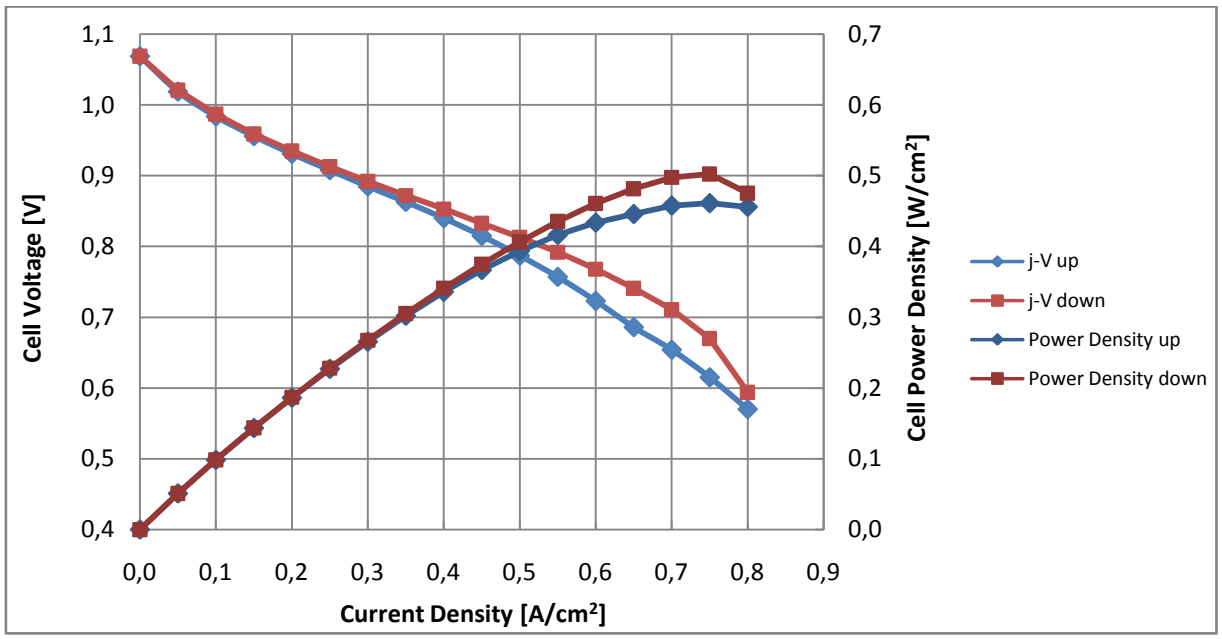

Figure 6.2.1 j-V and Power Density curves for cell temperature 800 °C (42 Nl/h of H_2; 100 Nl/h of Air).

This was the first test performed according to FCTESTNET procedure. It was done strictly according to the procedure. Two j-V curves visible on the graph show the cell response to the increasing ("j-V up") and decreasing ("j-V down") load. The difference occurs because of the cell temperature increase caused by high reaction rates during the high load. Compared to the value on the graph in InDEC ASC2 folder (see Appendix C), the OCV here is 1,069V (in the folder OCV is 1,04V). The voltage under 0,3 A/cm^2 current density (linear part of the plot) here is 0,892V (0,94V in InDEC folder). The result here was 5,1% lower than in the InDEC folder.

6.3 Test no. 2 (Cell temperature 750 °C)

Table 6.3.1 Gas feed parameters.

Gas type (MFC number)	**Flow rate Nl/h**
Air for cathode (03308004)	100
N_2 for anode (47400004)	0
H_2 for anode (47400003)	42 (Humidified at STP)
H_2 for anode (03308005)	0

Table 6.3.2 Test-rig parameters at test start.

Parameter	Value in °C
Cell Temp. (TC in the middle of the cathode)	736
Furnace Temp. (TC located in the Furnace space)	756
Average Cell Temperature	749,4

Results are presented on a graph (Figure 6.3.1 below). The tables with measurement results are included in Appendix B.

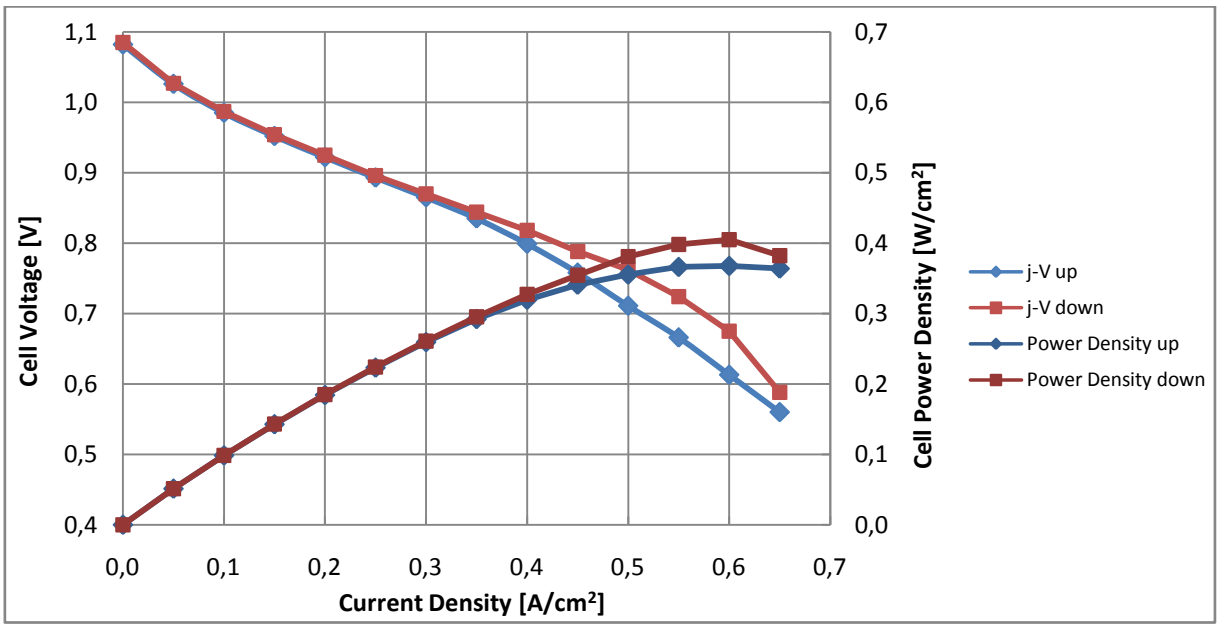

Figure 6.3.1 j-V and Power Density curves for cell temperature 750 °C (42 Nl/h of H_2; 100 Nl/h of Air).

According to the FCTESTNET suggestion, the test at 750 °C was conducted. The conclusions are the same as for the test at 800 °C. The maximum power density with increasing load (MPD up) was 20,2% lower than for 800 °C. The temperature dependence of the MPD will be discussed later in paragraph 6.8.1, page 54.

6.4 Test no. 3 (Cell temperature 700 °C)

Table 6.4.1 Gas feed parameters.

Gas type (MFC number)	Flow rate Nl/h
Air for cathode (03308004)	100
N_2 for anode (47400004)	0
H_2 for anode (47400003)	42 (Humidified at STP)
H_2 for anode (03308005)	0

Table 6.4.2 Test-rig parameters at test start.

Parameter	Value in °C
Cell Temp. (TC in the middle of the cathode)	691
Furnace Temp. (TC located in the Furnace space)	706
Average Cell Temperature	701

Results are presented on a graph (Figure 6.4.1 below). The tables with measurement results are included in Appendix B.

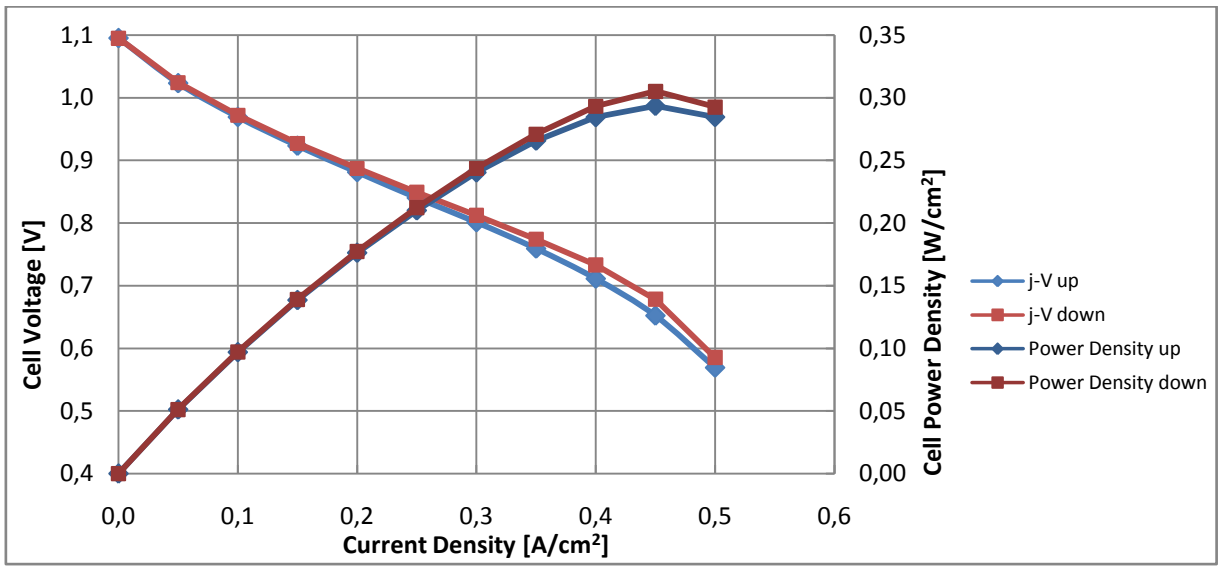

Figure 6.4.1 j-V and Power Density curves for cell temperature 700 °C (42 Nl/h of H_2; 100 Nl/h of Air).

According to the FCTESTNET suggestion, the test at 700 °C was conducted. The conclusions are again the same as for the test at 800 °C. The "MPD up" was 36,4% lower than for 800 °C. Compared to the value on the graph in InDEC ASC2 folder (see Appendix C), the OCV is here 1,095V (in the folder OCV is 1,075V). The voltage under 0,3 A/cm^2 current density (linear part of the plot) is here 0,812V (0,89V in InDEC folder). The result here was 8,8% lower than in the InDEC folder.

6.5 Test no. 4 (Cell temperature 850 °C)

Table 6.5.1 Gas feed parameters.

Gas type (MFC number)	Flow rate Nl/h
Air for cathode (03308004)	100
N_2 for anode (47400004)	0
H_2 for anode (47400003)	42 (Humidified at STP)
H_2 for anode (03308005)	0

Table 6.5.2 Test-rig parameters at test start.

Parameter	**Value in °C**
Cell Temp. (TC in the middle of the cathode)	836
Furnace Temp. (TC located in the Furnace space)	856
Average Cell Temperature	849,4

Results are presented on a graph (Figure 6.5.1 below). The tables with measurement results are included in Appendix B.

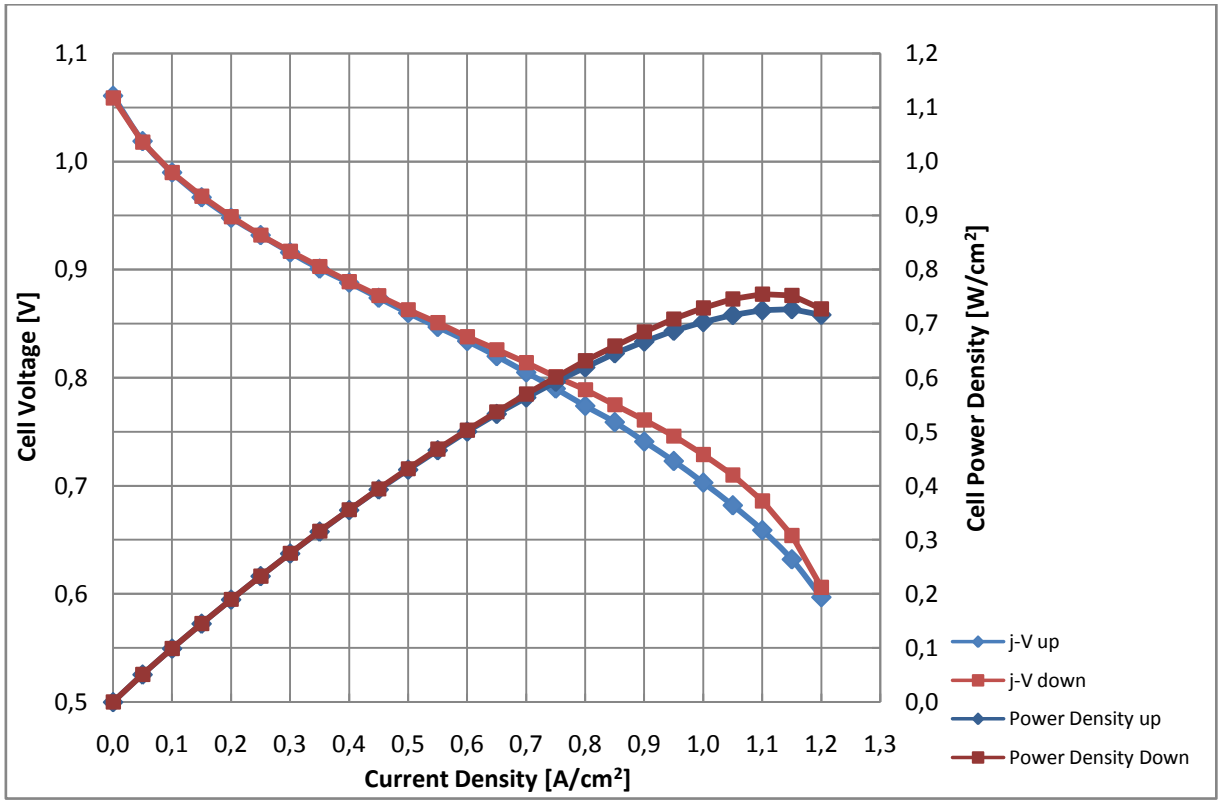

Figure 6.5.1 j-V and Power Density curves for cell temperature 850 °C (42 Nl/h of H_2; 100 Nl/h of Air).

According to the FCTESTNET suggestion, the test at 850 °C was conducted. The conclusions are again the same as for the test at 800 °C. The "MPD up" was 57,7% higher than for 800 °C.

6.6 Test no. 5 (Cell temperature 900 °C)

Table 6.6.1 Gas feed parameters.

Gas type (MFC number)	Flow rate Nl/h
Air for cathode (03308004)	100
N_2 for anode (47400004)	0
H_2 for anode (47400003)	42 (Humidified at STP)
H_2 for anode (03308005)	0

Table 6.6.2 Test-rig parameters at test start.

Parameter	Value in °C
Cell Temp. (TC in the middle of the cathode)	886
Furnace Temp. (TC located in the Furnace space)	905
Average Cell Temperature	898,7

Results are presented on a graph (Figure 6.6.1 below). The tables with measurement results are included in Appendix B.

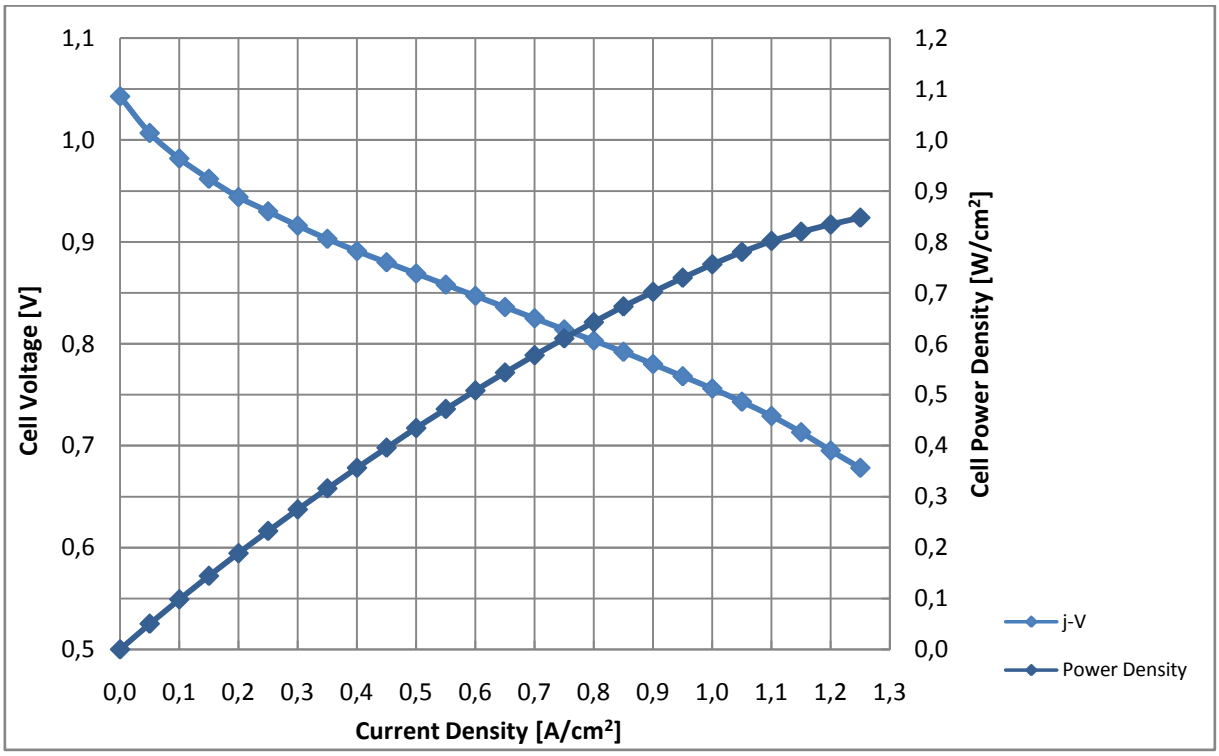

Figure 6.6.1 j-V and Power Density curves for cell temperature 900 °C (42 Nl/h of H_2; 100 Nl/h of Air).

Only increasing j-V curve was taken, because of safety reasons, with the high temperature and high reaction rates. Nevertheless this curve was taken according to FCTESTNET procedure. The first thing that we see is that the highest power density has not been achieved. But because the power density curve is almost flat we can take the last point as the MPD. It is 83,9% higher than for 800 °C.

6.7 Cool-down

After the last test the cool-down procedure was started according to the lab procedure. The cell was left at OCV, furnace was set to reach 20 °C with 27 °C/h cooling speed and the gas feed composition was immediately changed to anode – H_2 = 1,5 Nl/h and N_2 = 28,5 Nl/h, cathode – Air = 30 Nl/h.

After the cool-down finished, the cell was taken out and a picture of it was taken (see Figure 6.7.1 below).

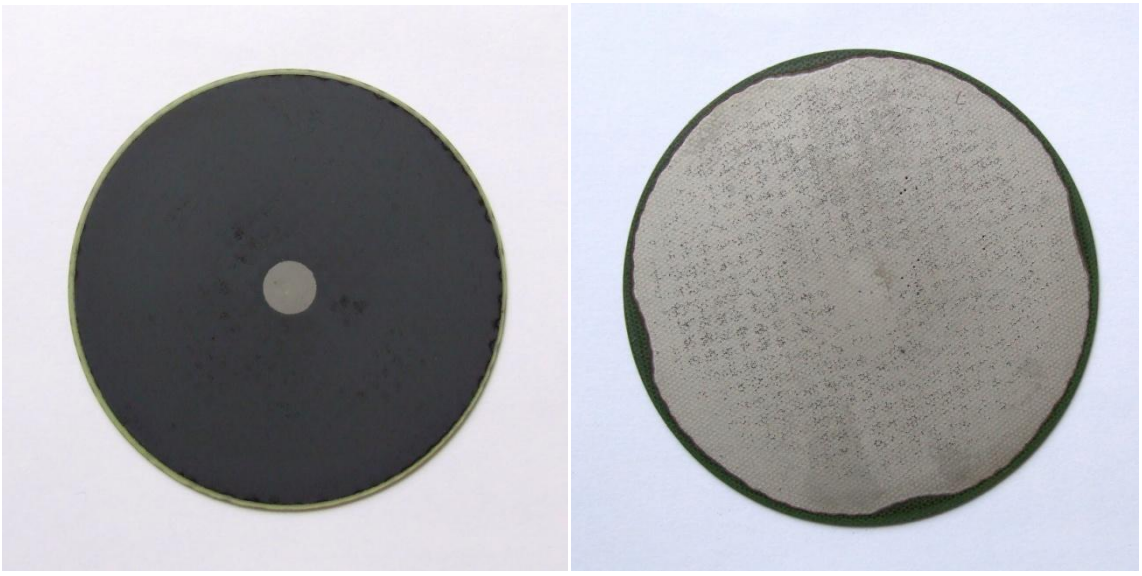

Figure 6.7.1 InDEC ASC2 Cell after the tests.

The cell is visually in a very good condition. The anode changed color to metallic (as usual) because of the presence of nickel.

6.8 Results discussion

6.8.1 Maximum Power Density point temperature dependence

As discussed before there is a strong dependence on the MPD value and the cell temperature. To investigate this dependence the "MPD up" was taken (it was obtained in the temperature closer to set point). The dependence is visible in Figure 6.8.1.

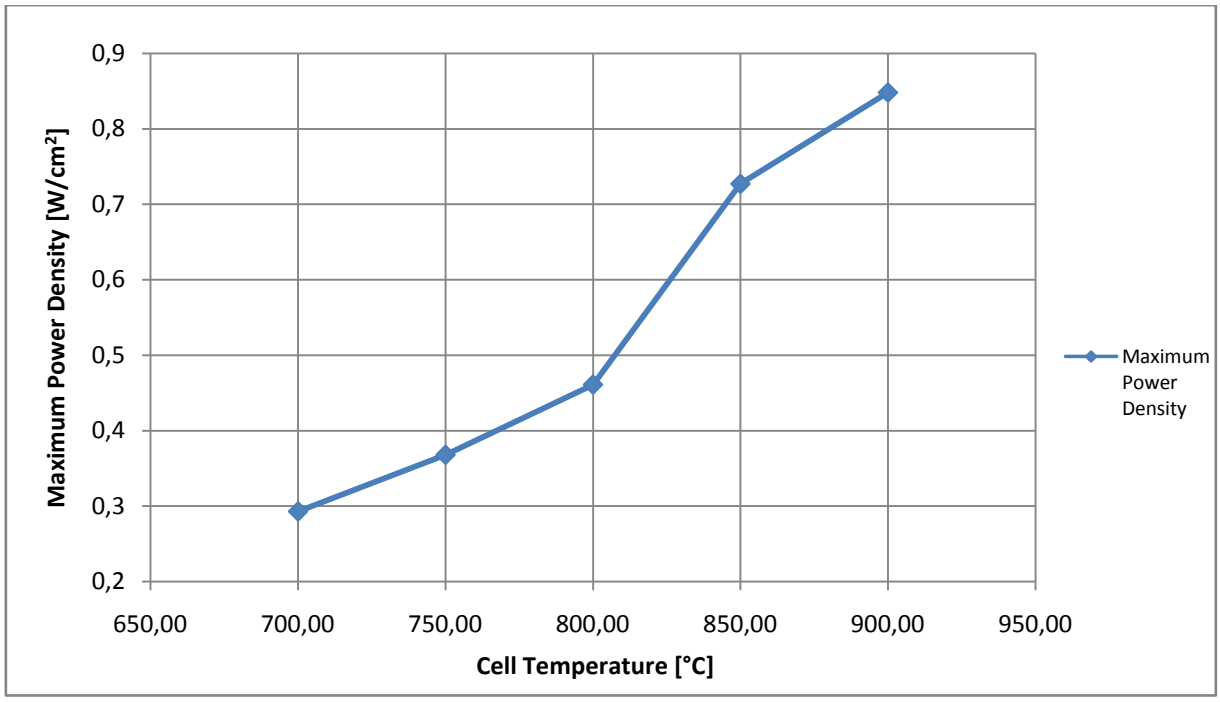

Figure 6.8.1 Maximum Power Density vs. Cell Temperature.

The curve visible on the graph can be roughly estimated by a straight line of the equation:

MPD = 0,0029 * Cell Temperature - 1,75

This equation shows that each 1 °C of temperature change changes the MPD of 0,0029 W/cm^2 which is 0,63% of MPD at 800 °C. It is a rough estimation of temperature influence on the cell performance.

6.8.2 Results discussion

A comparison should be done after presenting the particular results. Two comparisons were done:

Comparison of results obtained at 800 °C – the second (last) result of the start-up procedure and first test.

Figure 6.8.2 below shows the different polarization and power density curves obtained in temperature 800 °C.

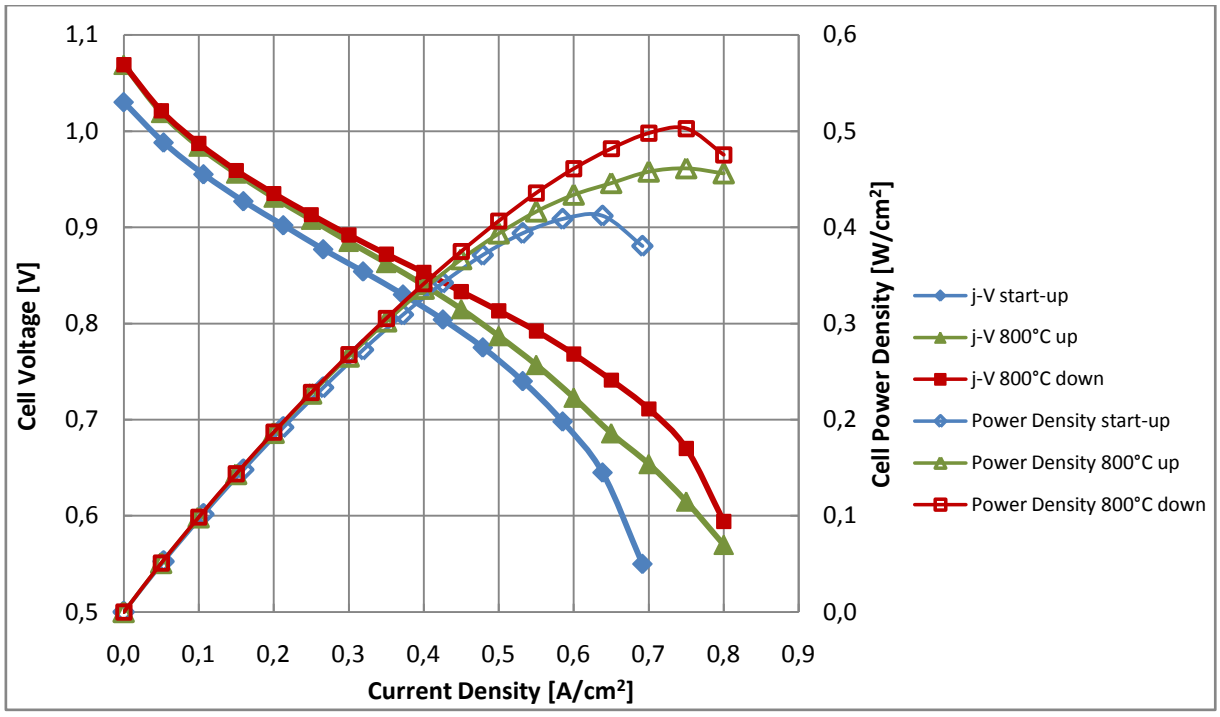

Figure 6.8.2 j-V and Power Density curves, temperature 800 °C.

It has to be noticed that during the start-up phase the test was conducted with different gas feed composition (24 Nl/h of H_2 + 60 Nl/h of Air) compared to the later test done according to FCTESTNET procedure (42 Nl/h of H_2 + 100 Nl/h of Air) lowered by 14,5%.

Comparison of ASC2 cell behavior with respect to temperature change.

This comparison should give perspective on the increase of the cell performance if the temperature is raised. The results are presented in two graphs for easier analysis (see Figure 6.8.3 and Figure 6.8.4 below). The graph containing both j-V and Power Density curves is attached to the work as Appendix A.

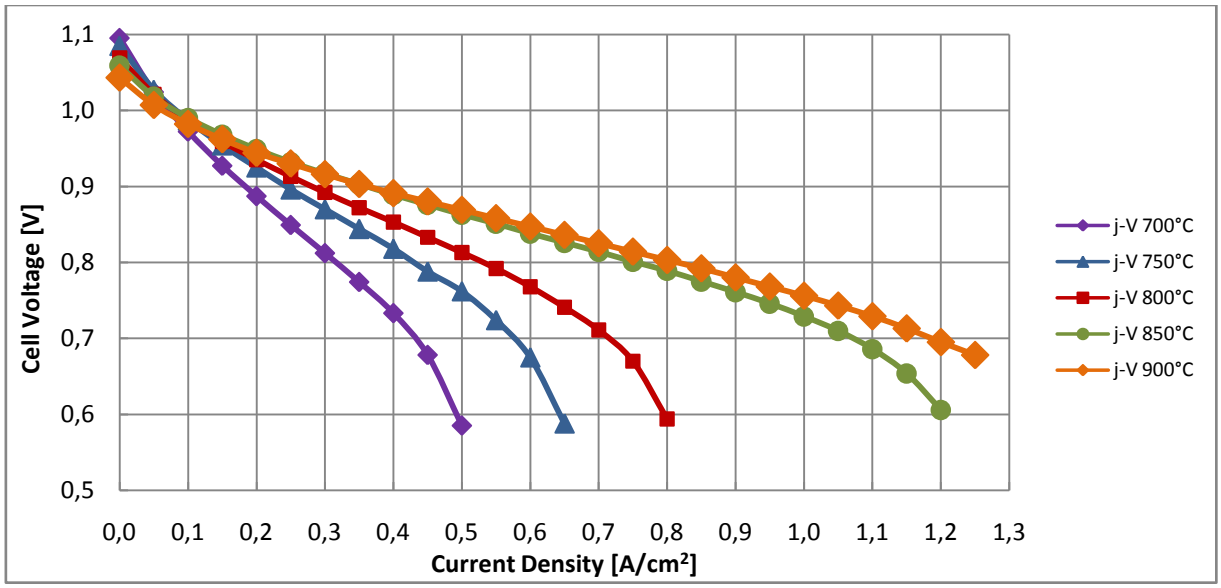

Figure 6.8.3 j-V curves at different temperatures.

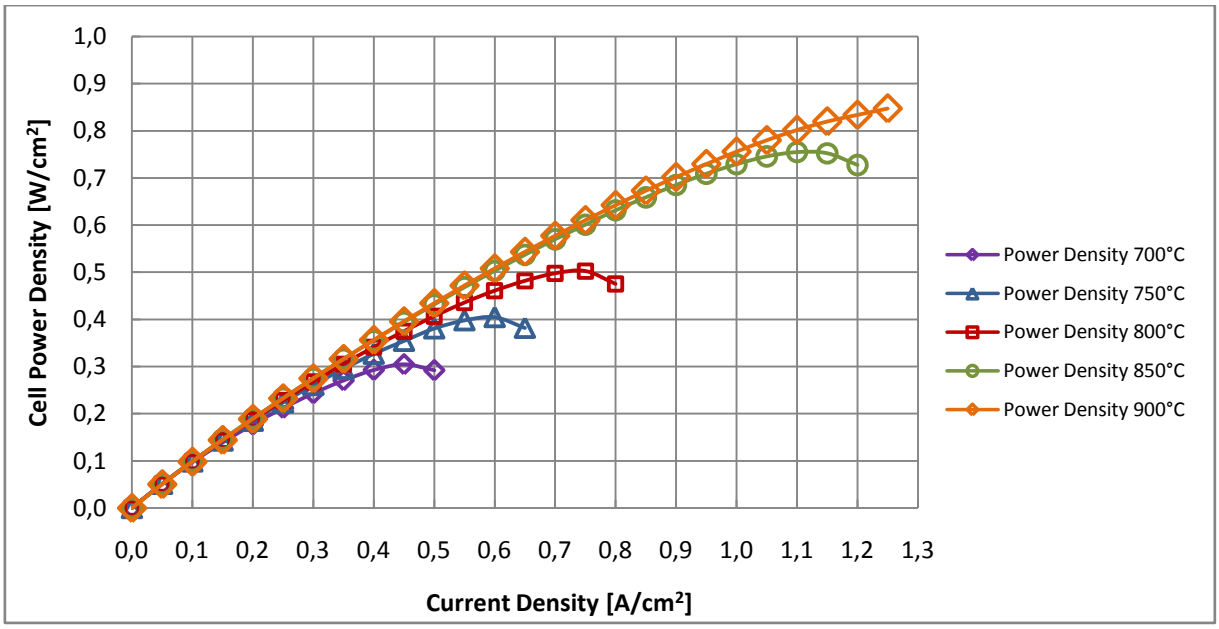

Figure 6.8.4 Power Density curves at different temperatures.

As a conclusion to the charts above it has to be stated that the cell operating temperature has a great influence on cell performance. The maximum power gained from the cell at 850 °C is twice the maximum power of the same cell at 700 °C. A similar relationship can be seen between this cell at 900 °C and 750 °C.

It can also be seen that because of some reasons the difference between cell performance at 850 °C and 900 °C is not that big. It may be caused by the fact that ASC2 cell was designed for so called intermediate operating temperatures (650 °C – 800 °C). Nevertheless it is easy to notice the performance boost gained from increasing the temperature from 800 °C to 850 °C.

A very interesting phenomenon is the drop of OCV of the cell with increasing temperature. It results from the drop of reversible thermodynamic voltage of the fuel cell with increasing temperature (see paragraph 5.4, page 43).

This drop in cell voltage is also caused by so called leakage current (Ryan O'Hayre et al. 2006, p. 171). It is a phenomenon of decreasing the area specific resistance (ASR) of the electrolyte with the increasing temperature. As an effect we get a short circuit (still of a high resistance, though) which shifts the j-V curve left. Unfortunately the result of this experiment shows these phenomena only qualitatively. The quantitative approach results in the conclusion that some value was not measured correctly: either the voltage of the cell or its temperature. The Open Circuit Voltage should be slightly lower than Reversible voltage (E_T) calculated in paragraph 5.4, page 43 but it is higher in each result (see Table 6.8.1 below).

Table 6.8.1 Reversible Thermodynamic Voltage vs OCV comparison.

Cell Temperature [°C]	**Reversible Thermodynamic Voltage [V]**	**OCV – results of the test [V]**
700	1,074	1,095
750	1,063	1,082
800	1,051	1,069
850	1,04	1,059
900	1,028	1,043

This looks like an error in measuring the temperature of the cell. Most probably the temperature values are lowered by some certain factor. The calibration of the thermocouples should be done with the new software but it was not.

It must be said that, especially in the regions of high current densities, the reaction rate is so fast that a shortage of fuel can occur in some places. Especially if we provided 14,5% less reactants than the FCTESTNET suggest. Therefore the results for high temperatures can be underestimated in the regions of high current density.

It cannot be stated that the results obtained from this cell are worse than the ones presented by InDEC B.V. in the folder (See appendix C). The temperature dependence of cells' performance and the temperature measuring uncertainty do not allow stating such a conclusion.

7 CONCLUSIONS

The main objectives of this work were to:

- Finish building the Single SOFC test bench.
- Create a "Single Solid Oxide Fuel Cell test bench model" that will allow time and gas consumption forecasting. The procedures for different tests should be included in this spreadsheet.
- Design the sulphur tolerance system (calculate the needed container H_2S in H_2 concentration and volume, choose the Mass Flow Controller for this mixture).
- Create an "Average Cell Temperature model".
- Read the recent scientific achievements in SOFC with special emphasis on single cells testing.
- Write necessary procedures (gas supply, start-up, PC and electronic devices configuration, applying weight, cool-down).
- Launch all parts of the test bench separately and finally launch the whole test bench and show that the procedures are written correctly.
- Perform the tests and drive the conclusions for future development of this test bench.

It is a part of a larger project that aims to investigate the influence of different fuel compositions and especially pollutants on SOFC performance, stability and durability.

The achievements of this work are:

- The SOFC test bench construction is finished, tests can be performed instantly.
- The "Single Solid Oxide Fuel Cell test bench model" has been created, used and proved to work very well. This model will be useful until the end of the ECN project in the FClab.
- The system responsible for sulphur tolerance tests was designed. It was calculated what kind of H_2S – H_2 mixture and what type of Mass Flow Controllers (MFCs) are needed to perform the sulphur tolerance tests. These parts (H_2 + 100 ppm of H_2S containers and a special MFC for this mixture) were already purchased and will be shipped shortly to the laboratory.
- The "Average Cell Temperature model" was performed and is a useful tool.
- 40 publications were studied (of which more than 25 were cited). The reason for this research was to deepen the understanding of processes occurring during fuel cell production and testing. I also realized the major trends of SOFC-related scientific development which are:
    - Different designs of the Solid Oxide Fuel Cells.
    - Development of the materials for electrodes and electrolyte.
    - Numerical modeling of SOFC.
    - SOFC Systems modeling and design

    - Performing SOFC single cells and stacks tests.
- It is very important to understand how the particular parts of the system work and share this knowledge with the future researchers that will work on this test bench. It is done by means of writing the detailed laboratory procedures. The procedures for gases supply initiation, start-up, applying weight on the cell, setting up the software and electronic devices and cool-down were written and shared with the laboratory staff (See appendix E).
- The procedures were validated during the first tests on the test-bench.
- Polarization tests were done in 5 different temperatures. The conclusions are in paragraph 0 starting on page 54.

The software is still in the development stage, but it allows saving data and works well enough to make the bench useful for SOFC testing. The future development of it in LabVIEW™ will result in one control panel that will allow controlling MFCs, data live on-screen presentation and acquisition and the electronic load control. Right now different software is used for controlling the flows.

The temperature measuring is a delicate point in this test bench. It should be deeply investigated and calibrated before the next tests.

It is also planned to include thermo-regulator control and the automation of start-up, cool-down and different tests procedures in the software's next generation. This would eliminate the possibility of human error.

Nevertheless we obtained the results that show the cell performance in different temperatures and the dependence of these two things is clearly visible. It has also been shown that the FCTESTNET procedures could be recommended as a way of making the tests of fuel cells. The results can now be presented to the others and there are no doubts as to how they were obtained.

The test bench is ready for further development. Possibly within a few months there will be other tests performed with introduction of different fuels and pollutants.

REFERENCES (ALPHABETICAL ORDER)

R.N. Basu, A. Das Sharma, Atanu Dutta, J. Mukhopadhyay, 2008, Processing of high-performance anode-supported planar solid oxide fuel cell, *International Journal of Hydrogen Energy*, vol. 33, pp. 5748 – 5754.

B.E. Buergler, M.E. Siegrist, L.J. Gauckler, 2005, Single chamber solid oxide fuel cells with integrated current-collectors, *Solid State Ionics*, vol. 176 pp. 1717 – 1722.

Tae Wook Eom, Hae Kwang Yang, Kyung Hwan Kim, Hyon Hee Yoon, Jong Sung Kim, Sang Joon Park, 2008, Effect of interlayer on structure and performance of anode-supported SOFC single cells, *Ultramicroscopy*, vol. 108, pp. 1283– 1287.

D. Herbstritt, et al., 1999, *Electrochem. Soc. 99*, vol. 19 pp. 972.

Ph. Hofmann, A. Schweiger, L. Fryda, K.D. Panopoulos, U. Hohenwarter, J.D. Bentzen, J.P. Ouweltjes, J. Ahrenfeldt, U. Henriksen, E. Kakaras, 2007, High temperature electrolyte supported Ni-GDC/YSZ/LSM SOFC operation on two-stage Viking gasifier product gas, *Journal of Power Sources*, vol. 173, pp. 357–366.

John P. Holdren, Sept. 1991, „Energy in transition", *Scientific American*, pp. 157-163.

Sadik Kakaç, Anchasa Pramuanjaroenkij, Xiang Yang Zhou, A review of numerical modeling of solid oxide fuel cells, *International Journal of Hydrogen Energy*, vol. 32, pp.761 – 786.

Timo Kivisaari, Pehr Björnbom, Christopher Sylwan, Bernard Jacquinot, Daniel Jansen, Arend de Groot, 2004, The feasibility of a coal gasifier combined with a high-temperature fuel cell, *Chemical Engineering Journal*, vol. 100, pp. 167–180.

Joon-Ho Koh, Young-Sung Yoo, Jin-Woo Park, Hee Chun Lim, 2002, Carbon deposition and cell performance of Ni-YSZ anode support SOFC with methane fuel, *Solid State Ionics*, vol. 149, pp. 157– 166.

Y.J. Leng, S.H. Chan, K.A. Khor, S.P. Jiang, 2004, Performance evaluation of anode-supported solid oxide fuel cells with thin film YSZ electrolyte, *International Journal of Hydrogen Energy*, vol. 29, pp. 1025 – 1033.

P. Leone, A. Lanzini, P. Squillari, P. Asinari, M. Santarelli, R. Borchiellini, M. Calí, 2008, Experimental evaluation of the operating temperature impact on solid oxide anode-supported fuel cells, *International Journal of Hydrogen Energy*, vol. 33, pp. 3167 – 3172.

Axel C. Müller, Dirk Herbstritt, Ellen Ivers- Tiffée, 2002, Development of a multilayer anode for solid oxide fuel cells, *Solid State Ionics*, vol. 152– 153, pp. 537– 542.

A.C. Müller, A. Weber, H.-J. Beie, A. Krügel, D. Gerthsen, E. Ivers- Tiffée, 1998, Proc. of 3rd European SOFC Forum, European Fuel Cell Forum, Oberrohrdorf, Switzerland, pp. 353– 362.

Futoshi Nishiwaki, Toru Inagaki, Jiro Kano, Jun Akikusa, Naoya Murakami, Kei Hosoi, 2006, Development of disc-type intermediate-temperature solid oxide fuel cell, *Journal of Power Sources*, vol. 157, pp. 809–815.

O'Hayre, R, Cha, SW, Colella, W & Prinz, FB (2006), *Fuel Cell Fundamentals*, John Wiley & Sons, New York.

T.L. Reitz, H. Xiao, 2006, *J. Power Sources*, vol. 161, pp. 437.

I. Riess, 2008, On the single chamber solid oxide fuel cells, *Journal of Power Sources*, vol. 175, pp. 325–337.

Gunter Schiller, Rudolf H. Henne, Michael Lang, Robert Ruckdaschel and Simone Schaper, n.d., Vacuum plasma sprayed thin-film SOFC for reduced operating temperature, *Fuel Cells Bulletin*, No.21 pp. 7-12.

Thorsteinn I. Sigfusson, (2008), *Planet Hydrogen - The Taming of the Proton*, Coxmoor publishing company, Oxford.

B.C.H. Steele, 1996, *Solid State Ionics*, vol. 86–88 (6S), pp. 1223.

André Weber, Ellen Ivers-Tiffée, 2004, Materials and concepts for solid oxide fuel cells (SOFCs) in stationary and mobile applications, *Journal of Power Sources*, vol. 127, pp. 273–283.

T. Weber, 1990, *Solid State Ionics*, vol. 42, pp. 205– 221.

Xianliang Huang, Hailei Zhao, Xue Li, Weihua Qiu, Weijiang Wu, July 2007, Performance of planar SOFCs with doped strontium titanate as anode materials, *Fuel Cells Bulletin.*

Xiao-Feng Ye, S.R. Wang, Z.R. Wang, L. Xiong, X.F. Sun, T.L. Wen, 2008, Use of a catalyst layer for anode-supported SOFCs running on ethanol fuel, *Journal of Power Sources*, vol. 177, pp. 419–425.

Y. Xiao-Feng, H. Bo, S.R.Wang, Z.R.Wang, L. Xiong, T.L.Wen, 2007, *J. Power Sources*, vol. 164 pp. 203–209.

SUN Xueli , LI Song, and SUN Juncai, Sept. 2006, Solid-state synthesis and electrochemical properties of $SmVO_4$ cathode materials for low temperature SOFCs, *Rare Metals*, Vol. 25, Spec. Issue, pp. 240.

Kyung Joong Yoon, Peter Zink, Srikanth Gopalan, Uday B. Pal, 2007, Polarization measurements on single-step co-fired solid oxide fuel cells (SOFCs), *Journal of Power Sources*, vol. 172, pp. 39–49.

Z. Zhan, S.A. Barnett, 2005, *Solid-State Ionics*, vol. 176, pp. 871–879.

Energy research Centre of the Netherlands (ECN) – public info, accessed on 27th Jan. 2009, <http://www.ecn.nl/en/corp/>.

Fuel Cell Systems Testing, Safety & Quality Assurance (FCTESQA) - Project Summary, accessed on 4th Nov. 2008, <http://fctesqa.jrc.ec.europa.eu/>.

APPENDIX A

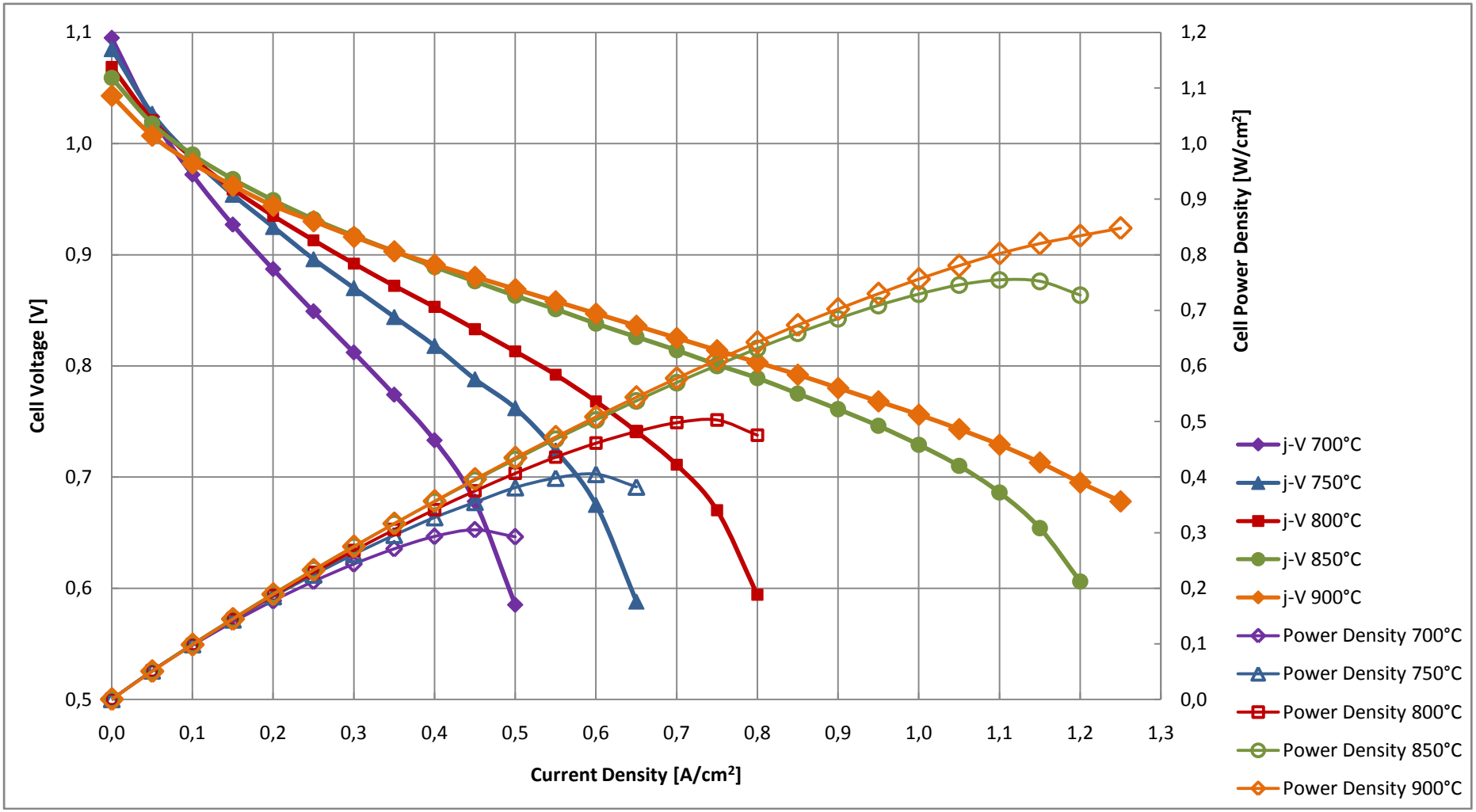

j-V and Power Density curves at different temperatures for ASC2.

APPENDIX B

7.1 Saturday 24th and Monday 26th January 2009, Start-up, Average Cell Temperature (ACT) 800 °C, 60 Nl/h of Air, 24 Nl/h of Hydrogen (humidified at STP)

Table 7.1.1 Start-up results, j-V curve number 1 (before 48h stabilization period).

Current [A]	Current density [A/cm^2]	Cell Voltage [V]	Power density [W/cm^2]
0	0,000	1,038	0,000
2,5	0,053	0,980	0,052
5,0	0,106	0,937	0,100
7,5	0,160	0,901	0,144
10,0	0,213	0,869	0,185
12,5	0,266	0,837	0,223
15,0	0,319	0,807	0,258
17,5	0,372	0,779	0,290
20,0	0,426	0,746	0,317
22,5	0,479	0,711	0,340
25,0	0,532	0,674	0,359
27,5	0,585	0,633	0,370
30,0	0,638	0,576	0,368
32,5	0,691	0,497	0,344

Table 7.1.2 Start-up results, j-V curve number 2 (after 48h stabilization period).

Current [A]	Current density [A/cm^2]	Cell Voltage [V]	Power density [W/cm^2]
0	0,000	1,030	0,000
2,5	0,053	0,988	0,053
5,0	0,106	0,955	0,102
7,5	0,160	0,927	0,148
10,0	0,213	0,902	0,192
12,5	0,266	0,877	0,233
15,0	0,319	0,854	0,273
17,5	0,372	0,830	0,309
20,0	0,426	0,804	0,342

22,5	0,479	0,775	0,371
25,0	0,532	0,740	0,394
27,5	0,585	0,698	0,408
30,0	0,638	0,645	0,412
32,5	0,691	0,55	0,380

7.2 Monday 26th January 2009, ACT 800 °C, 100 Nl/h of Air, 42 Nl/h of Hydrogen (humidified at STP)

Table 7.2.1 Results for increasing current density, 800 °C.

Current [A]	Current density [A/cm^2]	Cell Voltage [V]	Power density [W/cm^2]
0,00	0,000	1,069	0,000
2,35	0,050	1,019	0,051
4,70	0,100	0,984	0,098
7,05	0,150	0,956	0,143
9,40	0,200	0,931	0,186
11,75	0,250	0,908	0,227
14,10	0,300	0,885	0,266
16,45	0,350	0,863	0,302
18,80	0,400	0,840	0,336
21,15	0,450	0,815	0,367
23,50	0,500	0,787	0,394
25,85	0,550	0,757	0,416
28,20	0,600	0,723	0,434
30,55	0,650	0,686	0,446
32,90	0,700	0,654	0,458
35,25	0,750	0,615	0,461
37,60	0,800	0,570	0,456

Table 7.2.2 Results for decreasing current density, 800 °C.

Current [A]	Current density [A/cm^2]	Cell Voltage [V]	Power density [W/cm^2]
0,00	0,000	1,069	0,000
2,35	0,050	1,021	0,051
4,70	0,100	0,987	0,099
7,05	0,150	0,959	0,144
9,40	0,200	0,935	0,187
11,75	0,250	0,913	0,228
14,10	0,300	0,892	0,268
16,45	0,350	0,872	0,305
18,80	0,400	0,853	0,341

21,15	0,450	0,833	0,375
23,50	0,500	0,813	0,407
25,85	0,550	0,792	0,436
28,20	0,600	0,768	0,461
30,55	0,650	0,741	0,482
32,90	0,700	0,711	0,498
35,25	0,750	0,670	0,503
37,60	0,800	0,594	0,475

7.3 Tuesday 27th January 2009, ACT 750 °C, 100 Nl/h of Air, 42 Nl/h of Hydrogen (humidified at STP)

Table 7.3.1 Results for increasing current density, 750 °C.

Current [A]	Current density [A/cm^2]	Cell Voltage [V]	Power density [W/cm^2]
0,00	0,000	1,082	0,000
2,35	0,050	1,026	0,051
4,70	0,100	0,985	0,099
7,05	0,150	0,952	0,143
9,40	0,200	0,922	0,184
11,75	0,250	0,893	0,223
14,10	0,300	0,865	0,260
16,45	0,350	0,835	0,292
18,80	0,400	0,799	0,320
21,15	0,450	0,758	0,341
23,50	0,500	0,711	0,356
25,85	0,550	0,666	0,366
28,20	0,600	0,613	0,368
30,55	0,650	0,560	0,364

Table 7.3.2 Results for decreasing current density, 750 °C.

Current [A]	Current density [A/cm^2]	Cell Voltage [V]	Power density [W/cm^2]
0,00	0,000	1,085	0,000
2,35	0,050	1,027	0,051
4,70	0,100	0,987	0,099
7,05	0,150	0,954	0,143
9,40	0,200	0,925	0,185
11,75	0,250	0,896	0,224
14,10	0,300	0,870	0,261
16,45	0,350	0,844	0,295
18,80	0,400	0,818	0,327
21,15	0,450	0,788	0,355
23,50	0,500	0,762	0,381
25,85	0,550	0,724	0,398

28,20	0,600	0,675	0,405
30,55	0,650	0,588	0,382

7.4 Tuesday 27th January 2009, ACT 700 °C, 100 Nl/h of Air, 42 Nl/h of Hydrogen (humidified at STP)

Table 7.4.1 Results for increasing current density, 700 °C.

Current [A]	Current density [A/cm^2]	Cell Voltage [V]	Power density [W/cm^2]
0,00	0,000	1,095	0,000
2,35	0,050	1,023	0,051
4,70	0,100	0,969	0,097
7,05	0,150	0,923	0,138
9,40	0,200	0,881	0,176
11,75	0,250	0,840	0,210
14,10	0,300	0,801	0,240
16,45	0,350	0,759	0,266
18,80	0,400	0,711	0,284
21,15	0,450	0,652	0,293
23,50	0,500	0,569	0,285

Table 7.4.2 Results for decreasing current density, 700 °C.

Current [A]	Current density [A/cm^2]	Cell Voltage [V]	Power density [W/cm^2]
0,00	0,000	1,095	0,000
2,35	0,050	1,024	0,051
4,70	0,100	0,972	0,097
7,05	0,150	0,927	0,139
9,40	0,200	0,887	0,177
11,75	0,250	0,849	0,212
14,10	0,300	0,812	0,244
16,45	0,350	0,774	0,271
18,80	0,400	0,733	0,293
21,15	0,450	0,678	0,305
23,50	0,500	0,585	0,293

7.5 Wednesday 28th January 2009, ACT 850 °C, 100 Nl/h of Air, 42 Nl/h of Hydrogen (humidified at STP)

Table 7.5.1 Results for increasing current density, 850 °C.

Current [A]	Current density [A/cm^2]	Cell Voltage [V]	Power density [W/cm^2]
0,00	0,000	1,061	0,000
2,35	0,050	1,019	0,051
4,70	0,100	0,990	0,099
7,05	0,150	0,967	0,145
9,40	0,200	0,948	0,190
11,75	0,250	0,932	0,233
14,10	0,300	0,916	0,275
16,45	0,350	0,901	0,315
18,80	0,400	0,888	0,355
21,15	0,450	0,874	0,393
23,50	0,500	0,860	0,430
25,85	0,550	0,847	0,466
28,20	0,600	0,834	0,500
30,55	0,650	0,820	0,533
32,90	0,700	0,805	0,564
35,25	0,750	0,790	0,593
37,60	0,800	0,774	0,619
39,95	0,850	0,759	0,645
42,30	0,900	0,741	0,667
44,65	0,950	0,723	0,687
47,00	1,000	0,703	0,703
49,35	1,050	0,682	0,716
51,70	1,100	0,659	0,725
54,05	1,150	0,632	0,727
56,40	1,200	0,597	0,716

Table 7.5.2 Results for decreasing current density, 850 °C.

Current [A]	**Current density [A/cm^2]**	**Cell Voltage [V]**	**Power density [W/cm^2]**
0,00	0,000	1,059	0,000
2,35	0,050	1,018	0,051
4,70	0,100	0,990	0,099
7,05	0,150	0,968	0,145
9,40	0,200	0,949	0,190
11,75	0,250	0,932	0,233
14,10	0,300	0,917	0,275
16,45	0,350	0,903	0,316
18,80	0,400	0,889	0,356
21,15	0,450	0,876	0,394
23,50	0,500	0,863	0,432
25,85	0,550	0,851	0,468
28,20	0,600	0,838	0,503
30,55	0,650	0,826	0,537
32,90	0,700	0,814	0,570
35,25	0,750	0,801	0,601
37,60	0,800	0,789	0,631
39,95	0,850	0,775	0,659
42,30	0,900	0,761	0,685
44,65	0,950	0,746	0,709
47,00	1,000	0,729	0,729
49,35	1,050	0,710	0,746
51,70	1,100	0,686	0,755
54,05	1,150	0,654	0,752
56,40	1,200	0,606	0,727

7.6 Wednesday 28th January 2009, ACT 900 °C, 100 Nl/h of Air, 42 Nl/h of Hydrogen (humidified at STP)

Table 7.6.1 Results for increasing current density, 900 °C.

Current [A]	Current density [A/cm^2]	Cell Voltage [V]	Power density [W/cm^2]
0,00	0,000	1,043	0,000
2,35	0,050	1,007	0,050
4,70	0,100	0,982	0,098
7,05	0,150	0,962	0,144
9,40	0,200	0,944	0,189
11,75	0,250	0,930	0,233
14,10	0,300	0,916	0,275
16,45	0,350	0,903	0,316
18,80	0,400	0,891	0,356
21,15	0,450	0,880	0,396
23,50	0,500	0,869	0,435
25,85	0,550	0,858	0,472
28,20	0,600	0,847	0,508
30,55	0,650	0,836	0,543
32,90	0,700	0,825	0,578
35,25	0,750	0,814	0,611
37,60	0,800	0,803	0,642
39,95	0,850	0,792	0,673
42,30	0,900	0,780	0,702
44,65	0,950	0,768	0,730
47,00	1,000	0,756	0,756
49,35	1,050	0,743	0,780
51,70	1,100	0,729	0,802
54,05	1,150	0,713	0,820
56,40	1,200	0,695	0,834
58,75	1,250	0,678	0,848

APPENDIX C

Product Information

H.C. Starck HCST

InDEC B.V.

ASC2

Anode Supported Cell, type 2

Anode Support	Porous NiO/8YSZ	520 – 600 µm
Anode	Porous NiO/8YSZ	5 – 10 µm
Electrolyte	Dense 8YSZ	4 – 6 µm
Blocking Layer	YDC	2 – 4 µm
Cathode	Porous LSCF	20 – 30 µm

Typical geometrical qualification

Maximum Size	200 × 200 mm
Lateral Size Tolerance	± 0.1 mm
Total cell thickness	0.55 – 0.63 mm

Features

- SOFC cell suitable for intermediate temperature operation, 650 – 800 °C

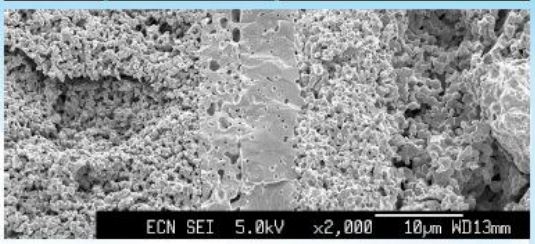

Typical electrochemical performance*

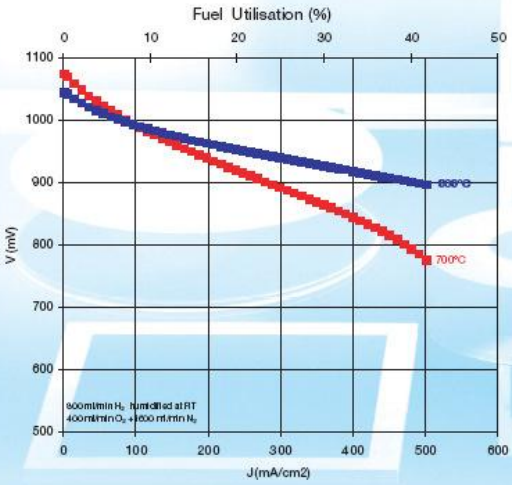

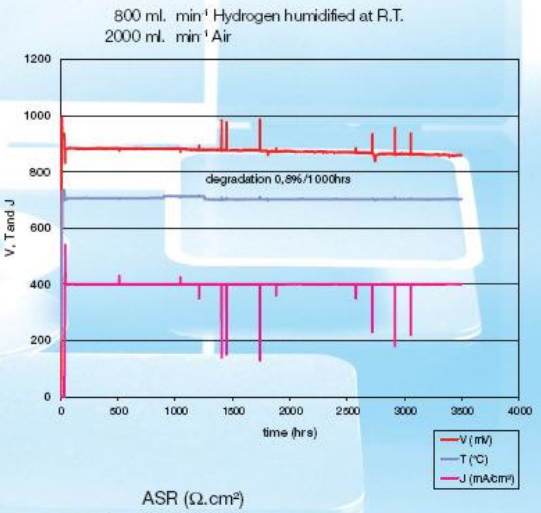

*Operating Conditions:

- Cell active area 100 cm²
- Ceramic single cell housing:
  Anode current collector Ni-grid
  Cathode current collector Pt-grid
- Non sealed cell housing

ASR (Ω.cm²)

500 hrs	0.47
1000 hrs	0.48
1500 hrs	0.49
2000 hrs	0.50

Abbreviations

ASC2	Anode Supported Cell, type 2	LSCF	Lanthanum Strontium Cobalt Ferrite Oxide
8YSZ	8 mol% Y_2O_3 doped ZrO_2	ASR	Area Specific Resistance
YDC	Yttria doped Ceria		

APPENDIX D

File name: 01-Cell Polarisation - H2 v0a.doc

SOFC cell polarisation curve with hydrogen

Measurement of the voltage as function of the current density and operating temperature as a generic measurement to evaluate the performance of SOFC cells with hydrogen.

Version..... 0

Test input..... Current density and temperature
Class of test input ..... Functional
Test output ..... Voltage
Class of test output ..... Functional

Class of test object..... Cell
Class of application .... Generic
Specific application .... None

Authors ..... Bert Rietveld
Revision date 19-01-2006

Revision history

Version	Change	Date	Status	Text / revision by
0		19-01-2006	Draft	Bert Rietveld
1				
2				
3				

Table of Contents

1 Objective and scope

Measurement of the voltage as function of the current density and operating temperature as a generic measurement to evaluate the performance of single SOFC cells with hydrogen.

This test is a general performance characterisation method for the research and development of SOFC cells.

2 Terminology, definitions and symbols

2.1 Terminology and definitions

Terminology and definitions used in this document are according to FCTESTNET terminology document.

Additional terminology and definitions are:

Cell area

- The (effective) cell area is defined as the area of the zone in which all cell components, that is anode, electrolyte and cathode, and the anode and cathode current collectors overlap.

2.2 Symbols

Symbols for physical quantities are defined in Handbook of Chemistry and Physics, 69th Edition, CRC Press. Below additional symbols are defined.

Symbol	Formula definition	Unit	Description
A_{cell}	Cell area	cm^2	Effective cell area
X_{fuel}		-	Volume composition of fuel
X_{ox}		-	Volume composition of oxidant
q_{fuel}	$q_{v,fuel}$ / A_{cell}	$ml.min^{-1}.cm^{-2}$	Volume flow of fuel per unit cell area (STP)
q_{ox}	$q_{v,fuel}$ / A_{cell}	$ml.min^{-1}.cm^{-2}$	Oxidant flow of fuel per unit cell area (STP)

3 Test Inputs

3.1 Variable Test Inputs

Input	Description	Range	Tolerance
J	Current density	0 - n* 0.05 - 1.25 $A.cm^{-2}$ *)	± 2% (rel)
	Hold time at current step	120 seconds	± 10 seconds (abs)
T	Operating temperature	400 - (n x 50) - 1050°C	± 5°C (abs)

*) Either this maximum current density or the limiting cell voltage of 0.6V

3.2 Static Test Inputs

Input	Description	Value	Tolerance (abs)
X_{fuel}	Fuel composition	97% H_2	Balance
		3% H_2O	± 1% H_2O
q_{fuel}	Fuel flow (STP)	18 $ml.min^{-1}.cm^{-2}$	± 1 $ml.min^{-1}.cm^{-2}$
X_{ox}	Oxidant composition	21% O_2 - 79% N_2	±1% O_2
q_{ox}	Oxidant flow (STP)	41.5 $ml.min^{-1}.cm^{-2}$	± 2 $ml.min^{-1}.cm^{-2}$

4 Test Outputs

Output	Description	Range	Accuracy	Sample Rate
V	Cell voltage	0.6 - 1.10 V	± 2% (rel)	> $1sec^{-1}$

5 References, Required Documentation and Provisions

5.1 References

5.2 Required documentation

1. FCTESTnet terminology document

5.3 Provisions

Standard local safety precautions for working with H_2 should be respected.

6 Test equipment and experimental set-up

This test procedure does not prescribe the geometry and size of the cell test housing.

The materials of the single cell test housing should be:

- an inert ceramic material (e.g. Al_2O_3) for the cell housing
- a platinum cathode current collector
- a nickel anode current collector

The current collectors should directly contact the electrodes of the cells. No intermediate contact layers should be applied between the electrode and the grids.

It is recommended to apply mesh type current collectors, preferably double grids at both the anode and the cathode side of the cell. The fine grid (e.g. wire diameter of 0.040 mm, 3600 $meshes.cm^{-2}$) should contact the cell. The coarser grid (e.g. wire diameter of 0.25 mm, 100 $meshes.cm^{-2}$) should completely cover the finer grid. The current and voltage leads should be attached to the coarser grid.

The thermocouple for measuring the cell temperature should be as close as possible to the cell.

The test report should describe the materials, types and sizes of the current collectors, and the geometry and sizes of the cell test housing.

7 Test procedure

7.1 Pre-conditioning the cell

The applied mechanical clamping pressure of the cell should be according to the recommendations of the cell manufacturer or according to common practice at the testing organisation.

The start-up of the cell should occur according the procedure recommended by the cell supplier or by the procedure that is common practice at the testing organisation.

The stabilisation of the cell can be part of the start-up procedure. If this is not the case it is recommended to follow either:

a) The recommendation of the cell supplier
b) The common practice at the testing organisation
c) Galvanostatic operation of the cell at the selected operating temperature, at the gas conditions of *3.2*, for minimum 4 hours, at a current density of 0.3 $A.cm^{-2}$.

The actual testing temperature should be an integer multiple of 50°C. In case either procedure a) or b) has been used for stabilisation, a second stabilisation period of 2 hours galvanostatic operation at the gas conditions of *3.2* and a current density of 0.3 $A.cm^{-2}$ should be applied before the actual measurement is started. In case of stabilisation procedure c) the measurement is started immediately thereafter.

Applied conditions and procedure for start-up and stabilisation should be described in the report of the test result.

7.2 Recording of the polarisation curve

In case the polarisation measurement is done at only one operating temperature, this temperature should be at n x 50°C (n is an integer).

The recording of current-voltage curves is under galvanostatic control, starting at the open circuit voltage using a fixed current step size (50 $mA.cm^{-2}$) and holding time (180 seconds). Gas compositions, flow rates and the temperature are constant during the measurement.

At the higher current densities considerable heating of the cell may occur. Therefore, it is recommended to monitor the cell temperature during the complete measurement.

The characteristic value of the cell voltage at each current density step is taken as the average value over the last 5 seconds of each step.

It is recommended not allowing cell voltages lower than 0.6 V. When this value is yielded before getting at the maximum current density the scan should be stopped.

Once the maximum current density of 1.25 $A.cm^{-2}$ or the limiting cell voltage of 0.6 V has been achieved the measurement is stopped.

Optional
Instead of stopping the measurement at the maximum current density or the limiting cell voltage, the scan can be reversed applying the same step size and holding time.

7.3 Varying the operating temperature

It is recommended to perform the polarisation measurement at several operating temperatures. A minimum of three operating temperatures with a temperature difference of 50°C is recommended. In that case the first polarisation measurement is at the temperature (fulfilling the n x 50°C rule) closest to the one at which the start-up or stabilisation procedure was concluded.

After completion of the first polarisation curve measurement the cell is brought to the nearest lower temperature. It is recommended to perform the temperature ramp at OCV.

At the new operating temperature, a stabilisation period of 2 hours at 0.3 $A.cm^{-2}$ and at the gas conditions of *3.2* is applied, after which the next procedure for recording the polarisation curve as described in 7.2 is executed.

The procedure of stabilisation and polarisation curve recording is repeated at the next 50°C lower temperature.

After the measurement has been performed at the lowest temperature, the temperature is ramped up to a temperature 50°C higher compared to the one of the first polarisation curve measurement. After the prescribed stabilisation procedure the polarisation curve after 7.2 is recorded.

The next polarisation curve measurement will be at a 50°C higher temperature.

Example.
Suppose the initial stabilisation was performed at 820°C. Then the temperature sequence at which the polarisation measurements are executed will be: 800 - 750 - 700 - 850 - 900°C.

8 Presentation of results

The presentation of the results should at least include:

- a description of the geometry and materials of the test housing: particularly the oxidant and fuel flow patterns
- a description of size and geometry of the cell
- the start-up procedure
- the stabilisation procedure
- the operating temperature of the test
- the statement that the test procedure described here has been applied and any intentional or accidental deviations from this procedure

or

- the actual test conditions: fuel composition and flow, oxidant composition and flow, current density

The polarisation data should be presented by both:

- A two-dimensional graph with the current density on the abscissa (x-axis) and the cell voltage on the ordinate (y-axis). Preferably the polarisation curves obtained at the various temperatures should be plotted in a single graph.
- A graph or table presenting the typical cell resistance at the applied operating temperatures, as calculated from the polarisation curves.
  - The cell resistance is defined by dV/dj at 0.7 V and is determined from the slope of the best fitting line over the measurement data within the interval 0.65 - 0.75 V.

Deviations from the prescribed procedure should be described in the report of the test result.

A proposed test result report is presented by Appendix A

Annex A Test report template

General information

Test module number		Test date	
Test version		Company performing test	
Company requesting test		Test location	
Test Request Nr		Test cell/equipment	

Test object description

Object manufacturer		Object weight [kg]	
Fuel cell technology		Object dimensions Length×Width×Height (cm^3)	
Object type		Object nominal power [W]	
Product number		Object peak power [W]	
Test object identification no.		Object voltage range [V]	

Test setup

Sketch the test setup, including sensor locations

Cell test housing

- Description of materials, grid types, geometry and sizes of the test housing.

Pre-conditioning of the cell

- Description of the start-up and stabilisation process.
- Applied mechanical clamping force.

Test procedure

- Reference to this test procedure.
- Any intentional or accidental deviations.

Results

- Two-dimensional graph comprising the polarisation curves at the various applied temperatures
- Table or graph presenting the area specific cell resistance (ASR) at the various test temperatures.

APPENDIX E

Cool-down procedure for a SOFC Single Cell

FC lab, Perugia, prepared by Marek Skrzypkiewicz

1. Set gas composition to:
    a. Anode:
        - Hydrogen 1,5 Nl/h,
        - Nitrogen 28,5 Nl/h;
    b. Cathode:
        - Air 30 Nl/h
2. On the furnace front panel labelled OGDEN ETR-9200

- do the following:
    a. Press button number 3, you will see the temperature the oven is set to (initially 800 °C will look like **0**800 <- green color) Notice the first "0" is highlighted
    b. Press button number 3 again to highlight the next digit, you will see 0**8**00
    c. Press and hold button 3 to change the number of hundreds. It will go down to 0, and then again from 9 (so it is not a problem if you miss the right number you want to set). Set the value to "0"
    d. After setting number of hundreds we want to set the decimal number: Press button number 3 again to highlight the decimal number
    e. Press and hold button number 3 to change the decimal number to 2
    f. If you see on the front panel the indication 00**2**0, the furnace is set correctly for cooling down the cell. After 12 seconds the front panel will switch to the temperature indication
3. Wait until the red temperature on the furnace front panel reach 20 °C (which takes 29 hours if the cool down starts at 800 °C and finishes at 20 °C) and turn the furnace off

Applying weight on SOFC procedure

FC lab, Perugia, prepared by Marek Skrzypkiewicz

1. Prepare air supply according to lab procedure
2. Set the air pressure regulator to 3 bar +/- 0,2 bar
3. Put the switch in the “up” position, the piston will move down

4. Observe the manometer pressure

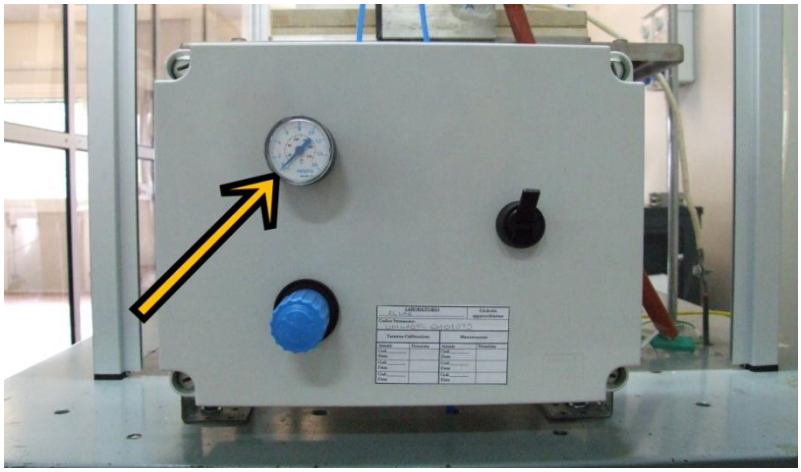

5. Using the blue regulator, set it to 0,5 bar for 4,5 kg or to 0,8 bar for 11 kg weight